Course B: rf technology
Normal conducting rf
Part 6: High-Gradient Acceleration

Walter Wuensch, CERN
Seventh International Accelerator School for Linear Colliders
1 to 4 December 2012

Now – acceleration with high gradient!

We are now going to look at what happens when you operate an rf structure at high-gradient and high-power.

To remind you of the CLIC parameters: the accelerating gradient is 100 MV/m with an input power of around 64 MW. PETS feed two accelerating structures so need to produce 130 MW.

High-power behavior is not described by a nice, clear theory, with proofs and theorems.

Instead what we have is picture emerging from the fog. I will describe the current understanding of how rf structures behave at high-power:
• How achievable gradient and power level depend on rf geometry.
• The physics of high-power phenomenon.
• Technology and why we think it works.

To do this I will cover:
1. Experiments and results.
2. Scaling laws
3. Physics of breakdown

A few more words of background.

A number of effects which emerge at high-power and high-gradient.

These include:

1. Breakdown – This is essentially the same phenomenon you all know from daily life, sparking and arcing. This is the main effect limiting gradient in CLIC.
2. Pulsed surface heating – Surface currents cause pulsed temperature rises, consequently cyclical stress which breaks up the surface and induces breakdown.
3. Electromigration – This is a new area of investigation in which rf currents directly affect the crystal structure of the copper surface.
4. Dark currents – Field emission currents are captured by the rf and can be accelerated over longer distances.
5. Dynamic vacuum – Field emission currents desorbs gasses which cause pressure rises during the rf pulse.
6. Multipactor – not really a problem at the highest gradients.

- What does a high-power rf test look like?
- What happens when an rf structure breaks down?

The basic layout of an rf test

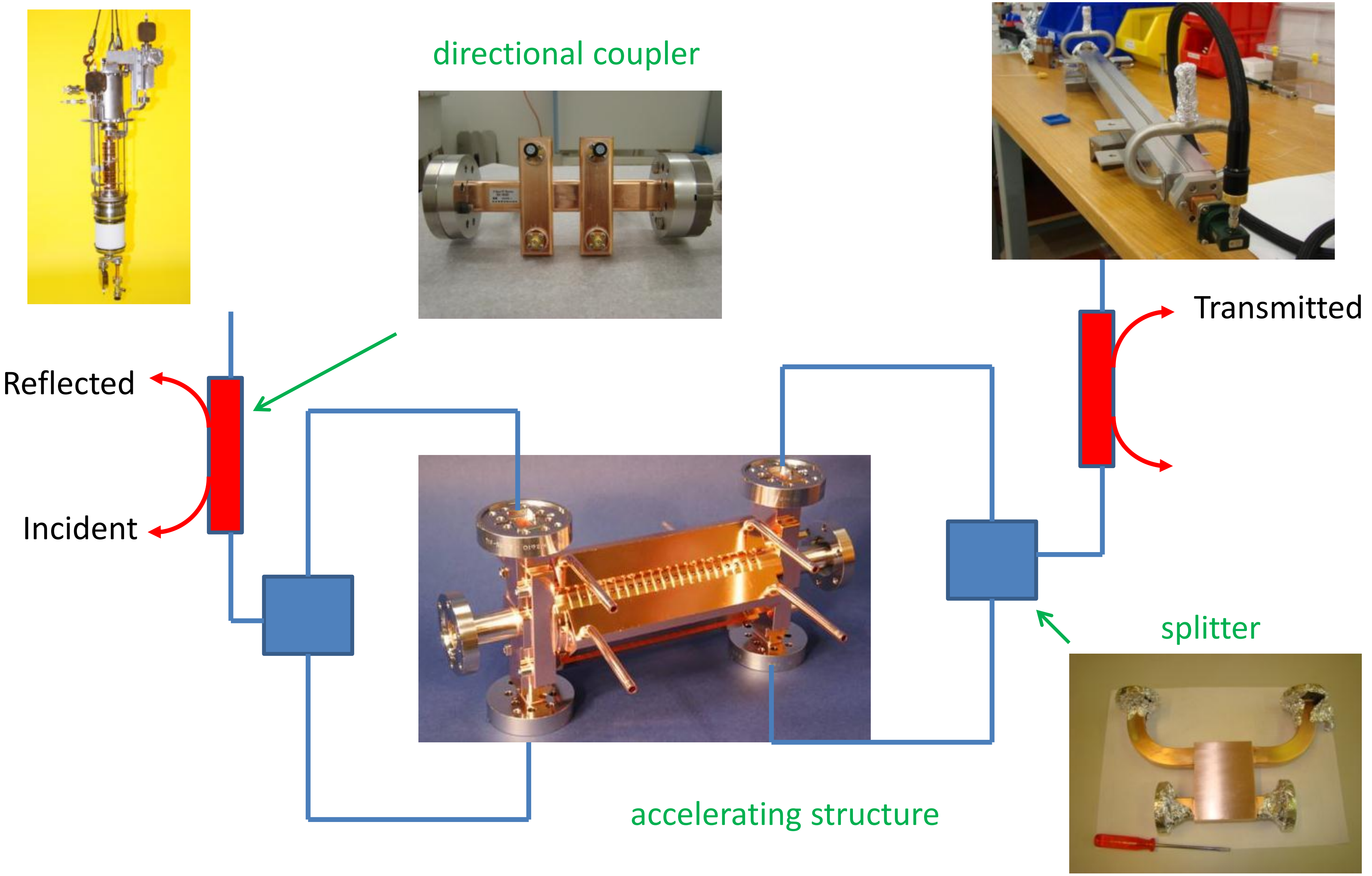

The basic layout of an rf test

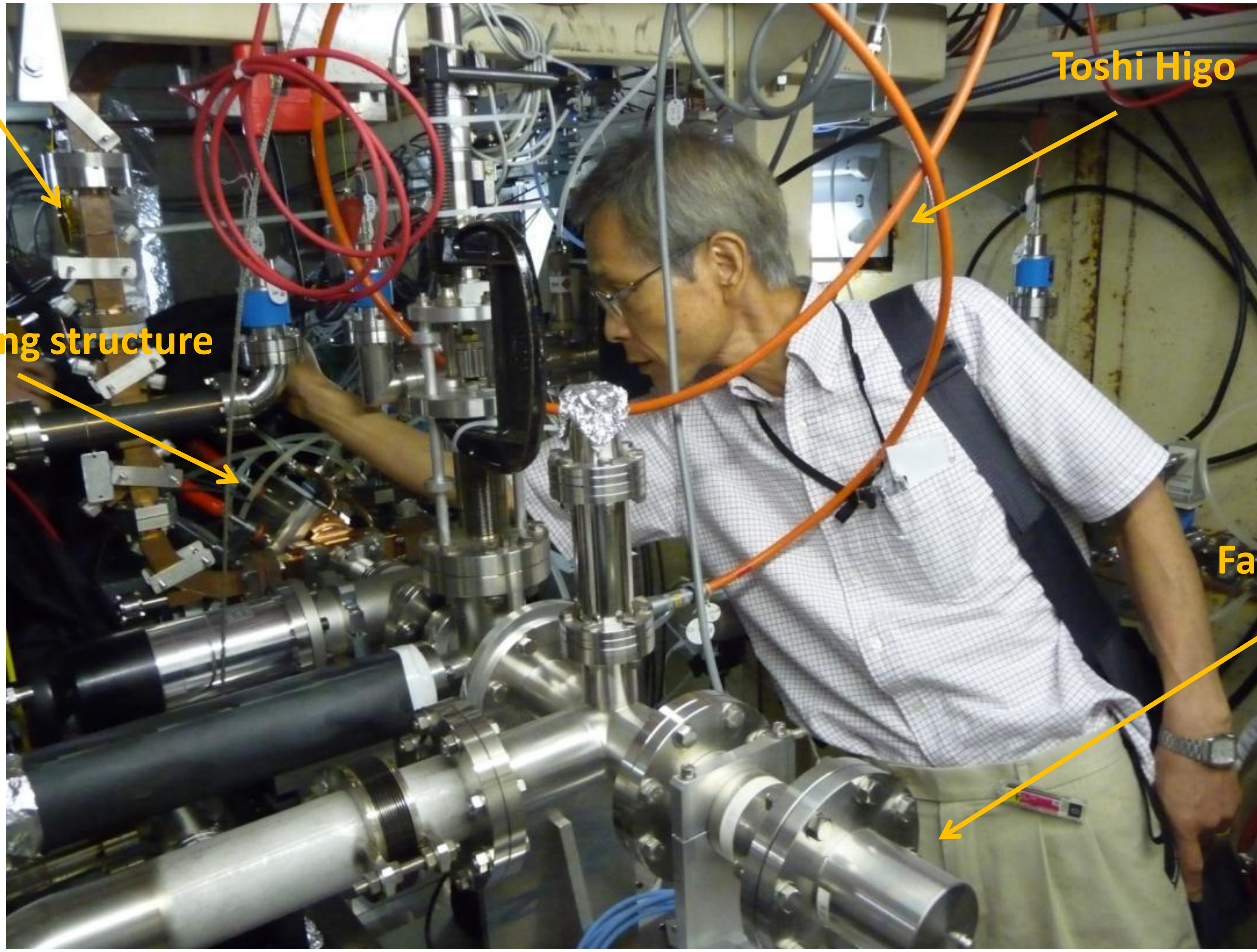

Prototype accelerating structure test areas

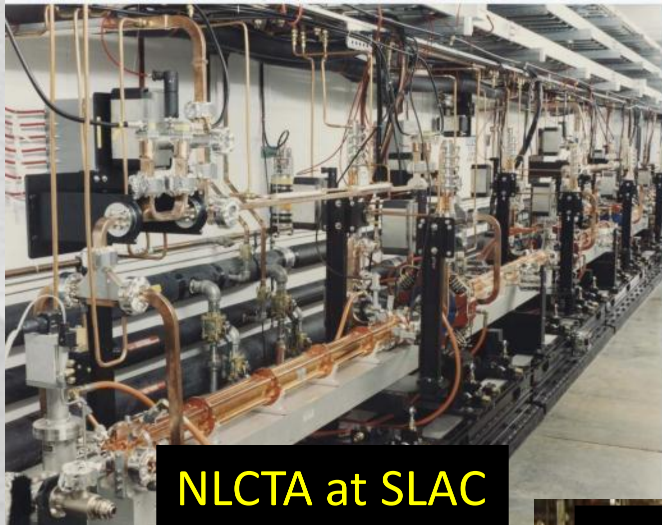
NLCTA at SLAC


Nextef at KEK


New klystron at CERN


ASTA at SLAC


Two-beam test stand at CERN

Layout of the CERN x-band test stand (X-box 1)

Clockwise from top-left:

- Modulator
- Pulse compressor
- DUT + connections
- Accelerating structure

Galler
y
Bunke
r

X-Box#2 at one of its possible location

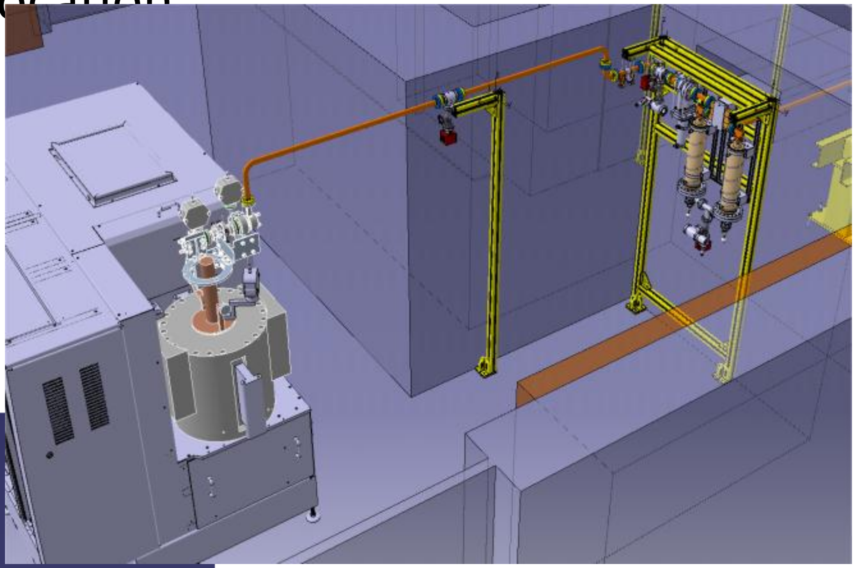

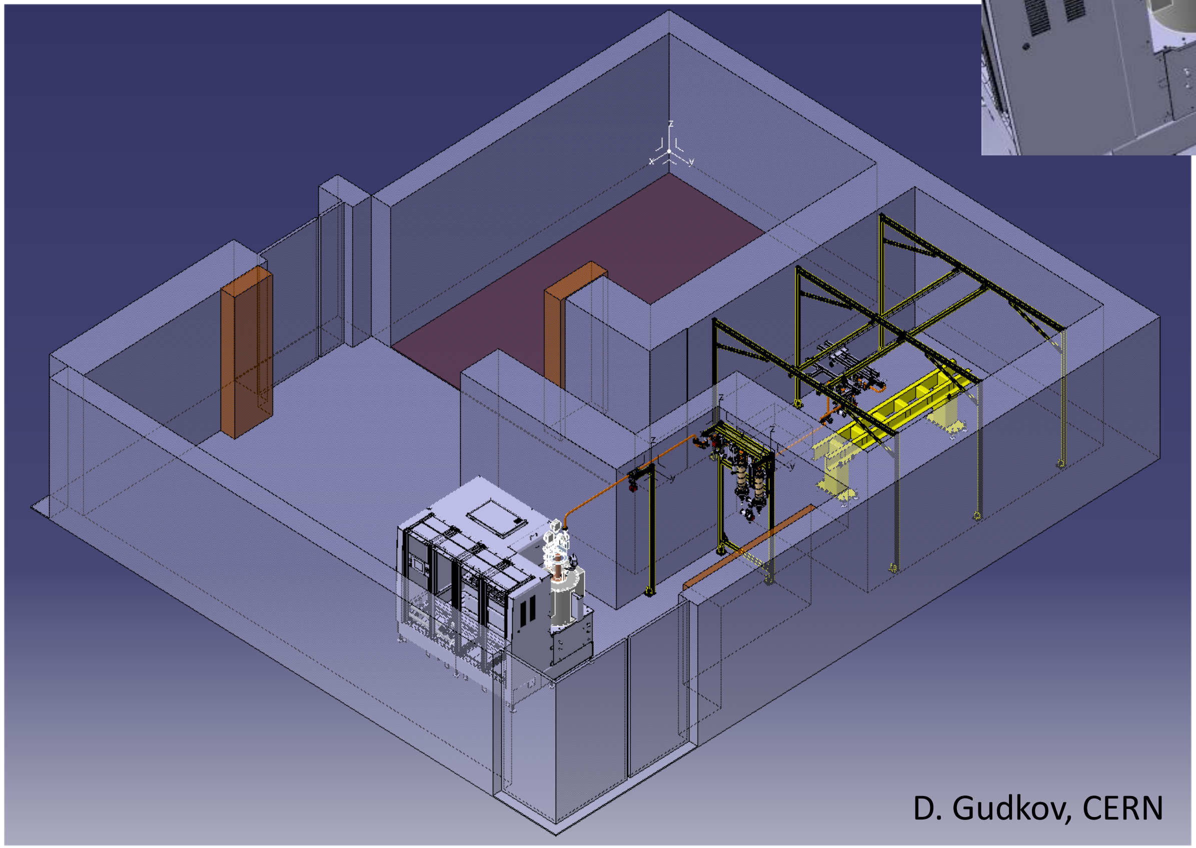

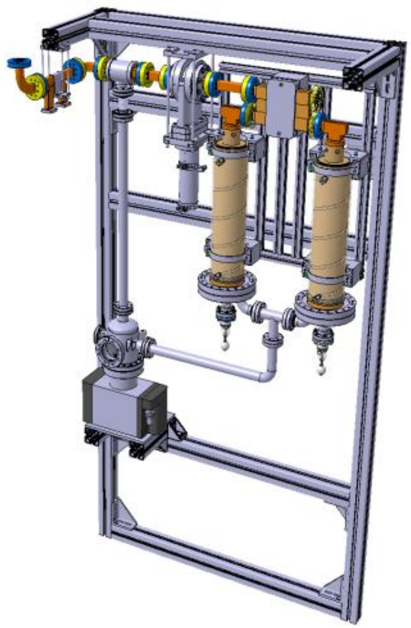

New X-box 1 DAQ system

Based on NI LabView and NI PXI hardware

50dB log detector into 14bit 250MSps/s ADC for controls

Last interlock event display (plus two previous pulses)

Interlock levels, calibration etc.

Power, DC, beta history

Single shot FN-plot

All at 50Hz rep. rate! 400Hz possible!

Development of improved DAQ system for Xbox 2

- Improve rf DAQ by using faster ADCs with higher dynamic range (1.6Gsps/s, 800MHz analogue BW)
- Decrease system complexity and calibration issues by using a down mixing and direct IF sampling scheme
- Low-level synthesis of driving rf signal with I/Q modulator and two 400Msps/s DACs allows very flexible pulse shaping
- Only one PXI crate for timing, interlocks, low level rf synthesis and rf data acquisition
- All interlocks as FPGA logic with watchdog and multiple instances gives high reliability
- Independent of CERN control system
- Operation at 400Hz repetition rate seems feasible

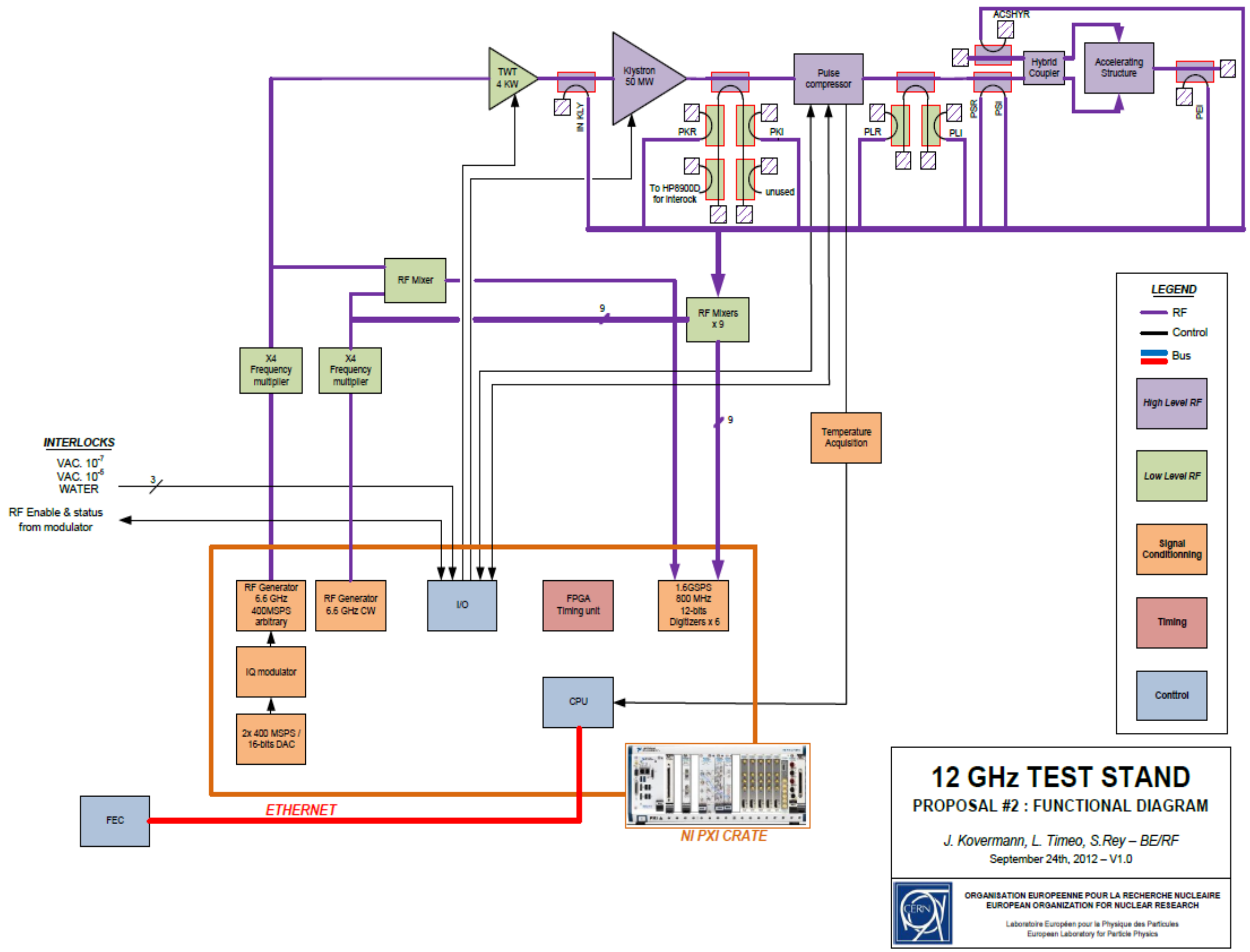

➔Proof of concept until beginning of 2013

Nextef expansion is being proceeded

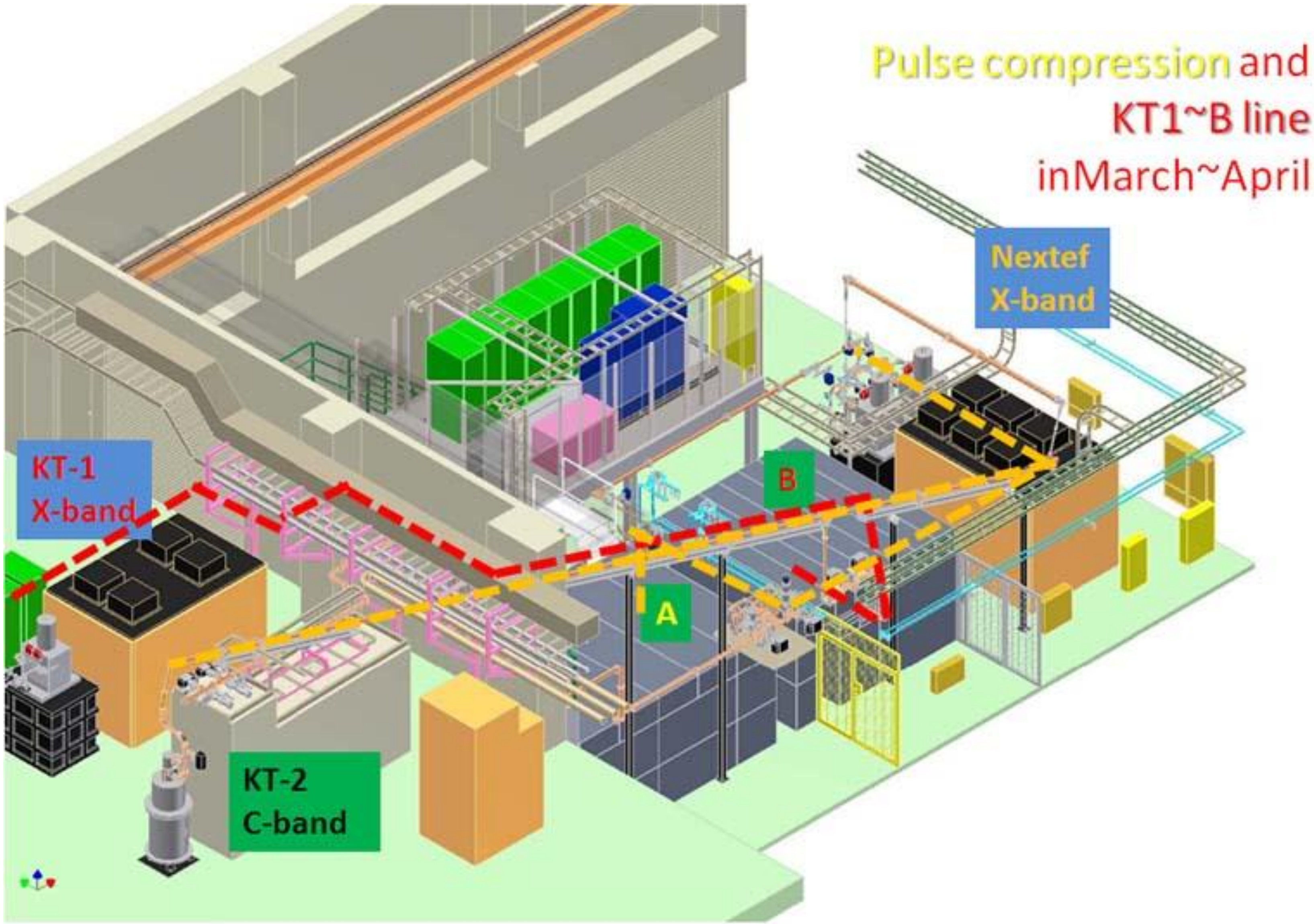

BD detection

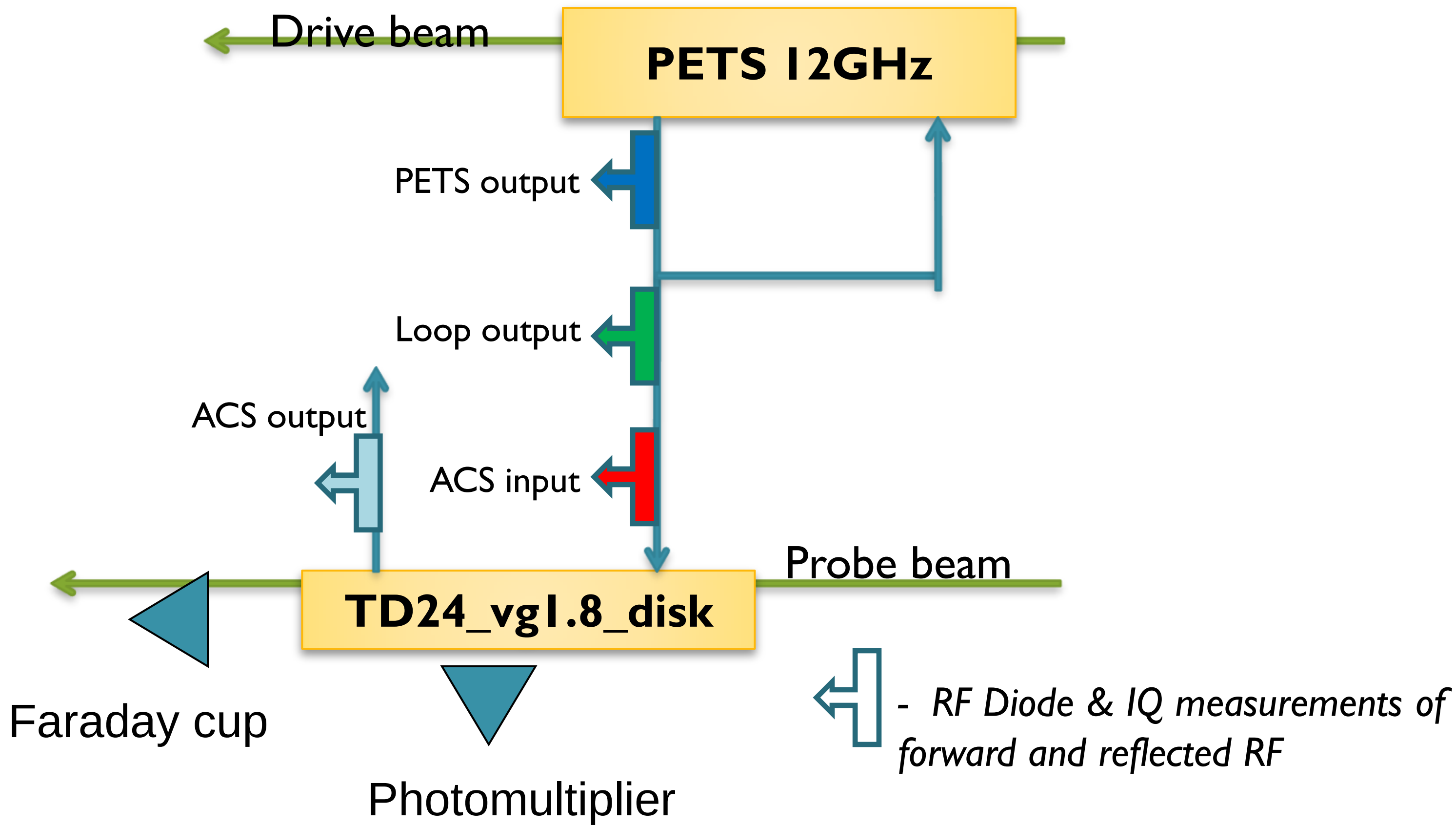

- Breakdowns in the recirculation loop are detected only from the reflected power (*Pref / Pfwd > ~15%*).
- Breakdowns in attenuator and the waveguide are detected from the missing energy (*Utran / (Ufwd * transmission factor) > 15%*)
- Breakdowns in the ACS are detected from the reflected power, the missing energy, the Faraday cup and the photomultiplier.

Acceleration

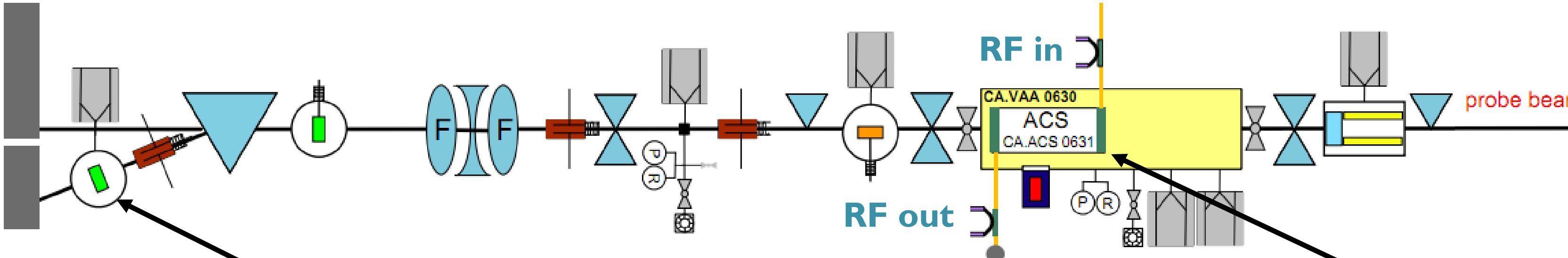

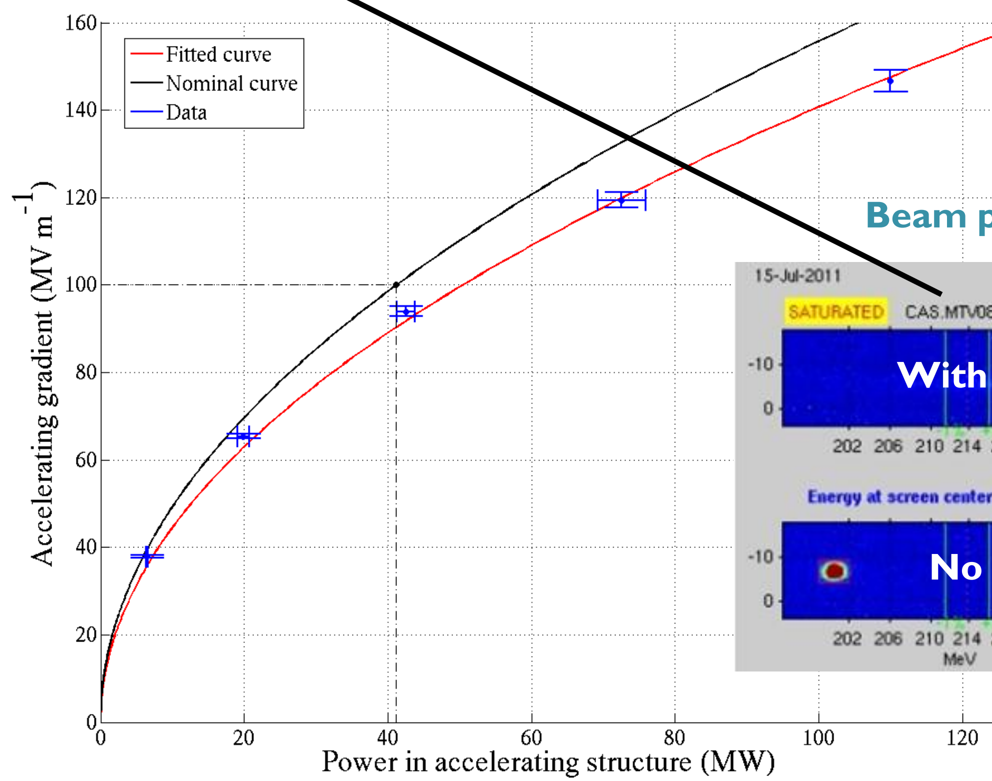

Beam profile monitor

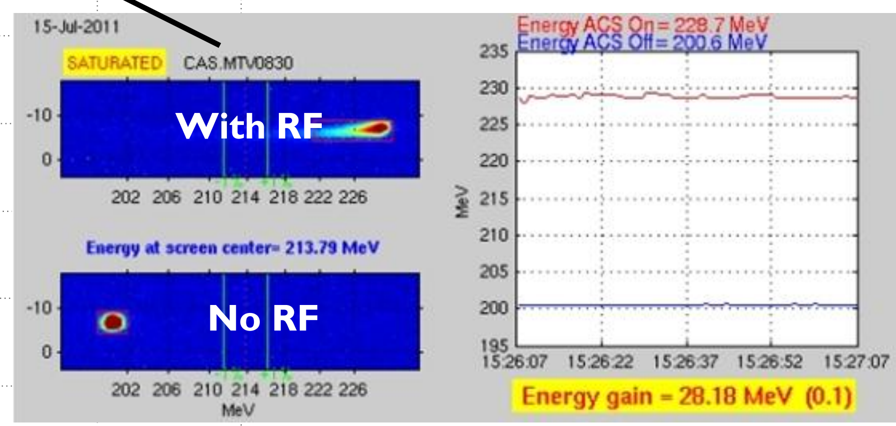

The acceleration of 145 MeV/m has been achieved.
(CLIC acc.g. is 100 MV/m)

51+52 Normal pulse #36

Incident (F)

Reflected (Rs)

Transmitted (Tr)

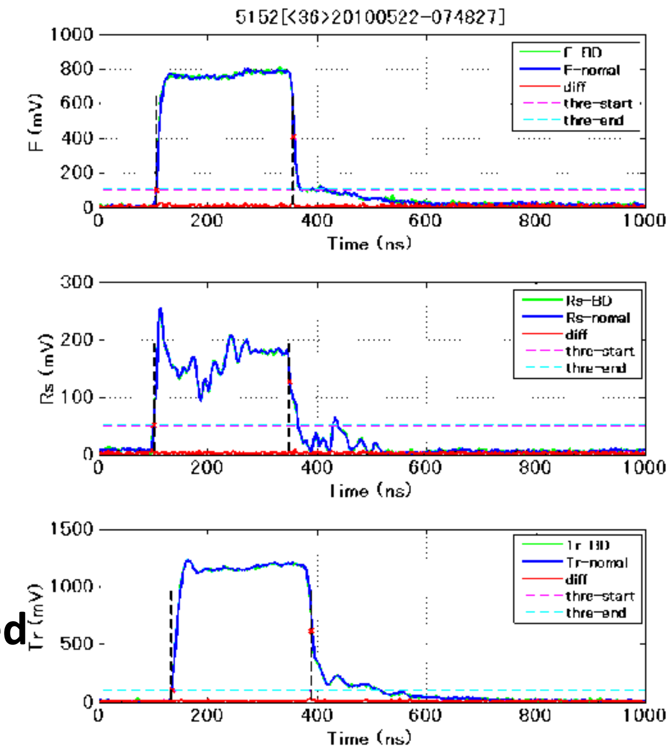

Last pulse

Last pulse but one

Difference between the two

Dashed lines = Analysis threshold

F RsX10 Tr

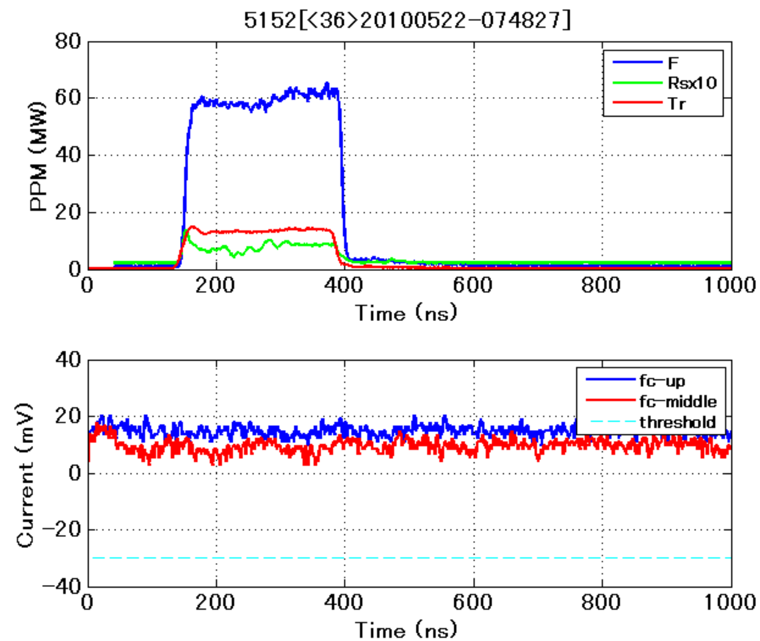

FC-UP FC-Mid Threshold

T. Higo, KEK
Test of TD18 structure

51+52 typical BD pulses
#72 Reflected RF back from klystron again

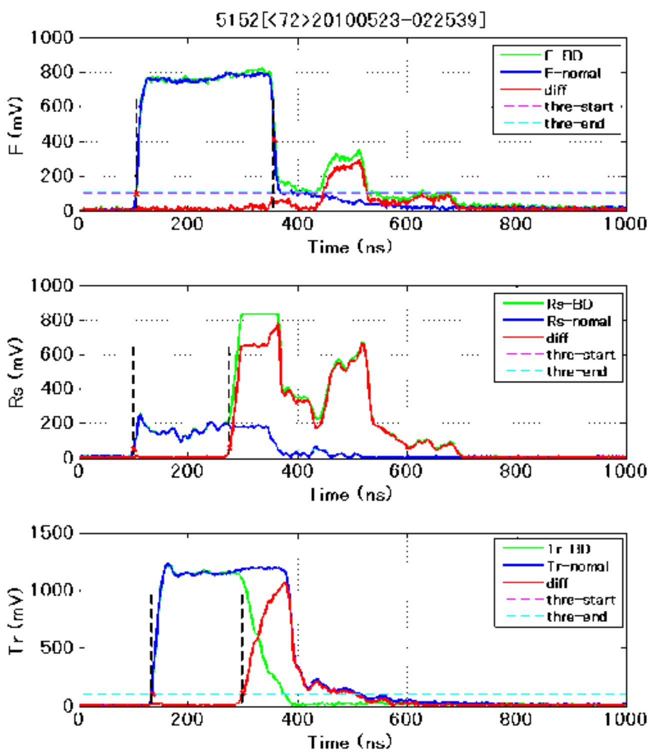

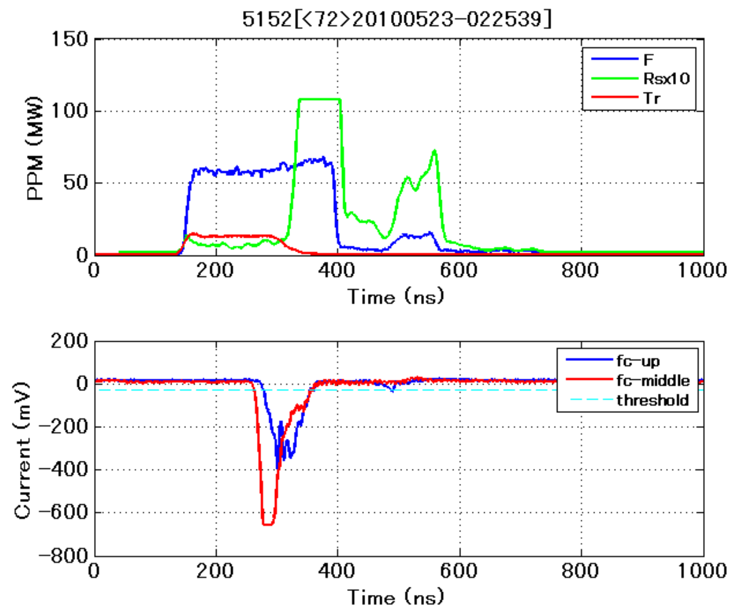

T. Higo, KEK
Test of TD18 structure

1: TW

Normal Waveforms of TD18 (s11 = -26.55 dB, s21 = -1.37 dB)

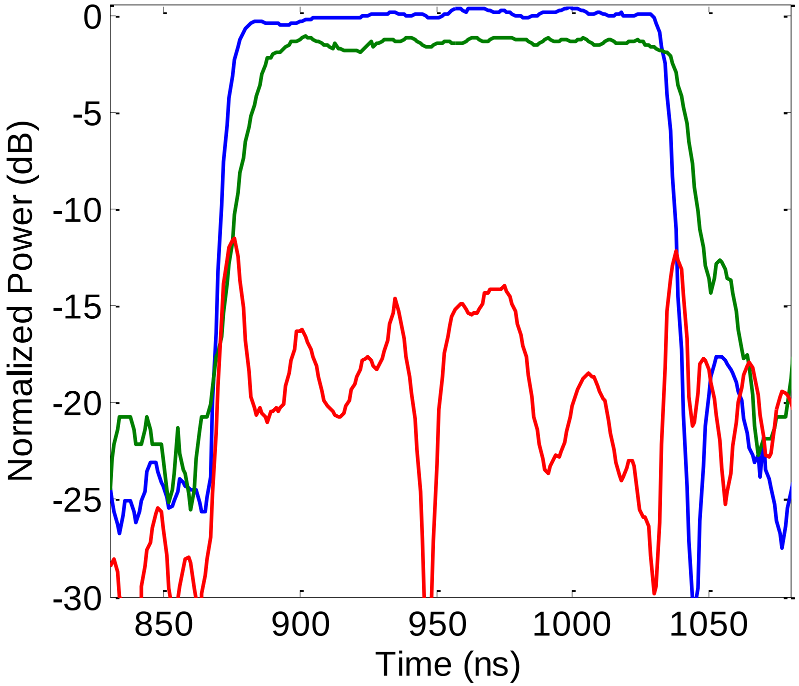

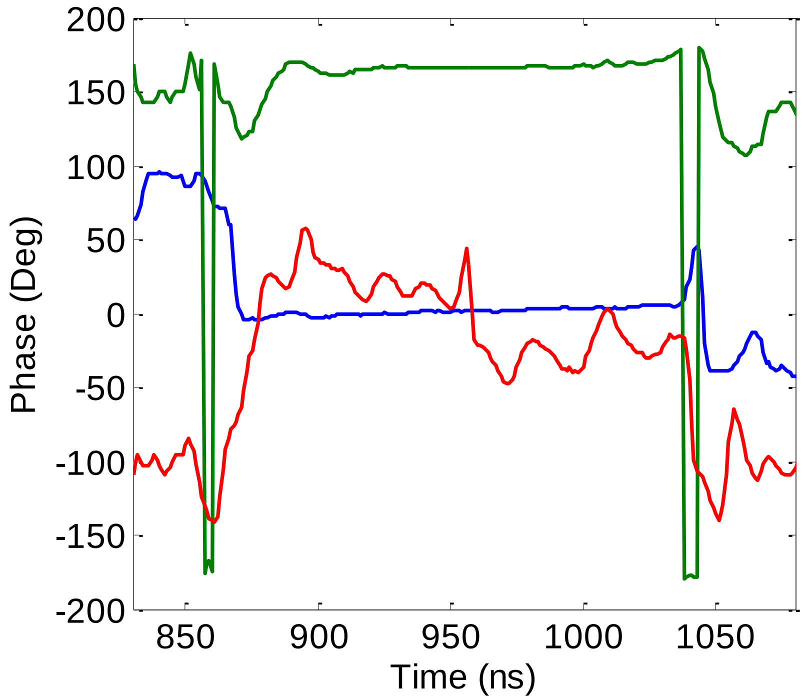

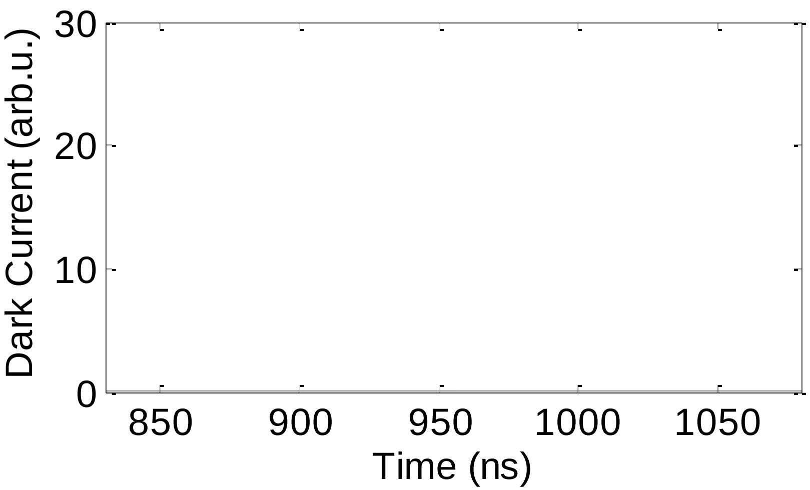

Blue – Input Forward, Green – Output Forward, Red – Input Reflected, Black – dark current.

F. Wang, SLAC
Test of TD18 structure

1: TW

Breakdown Waveforms of TD18

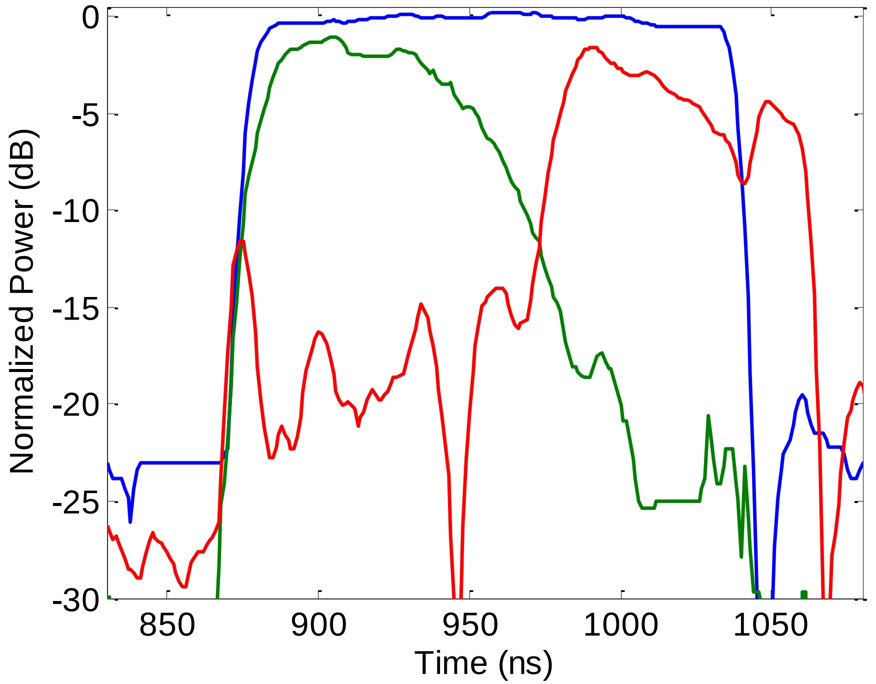

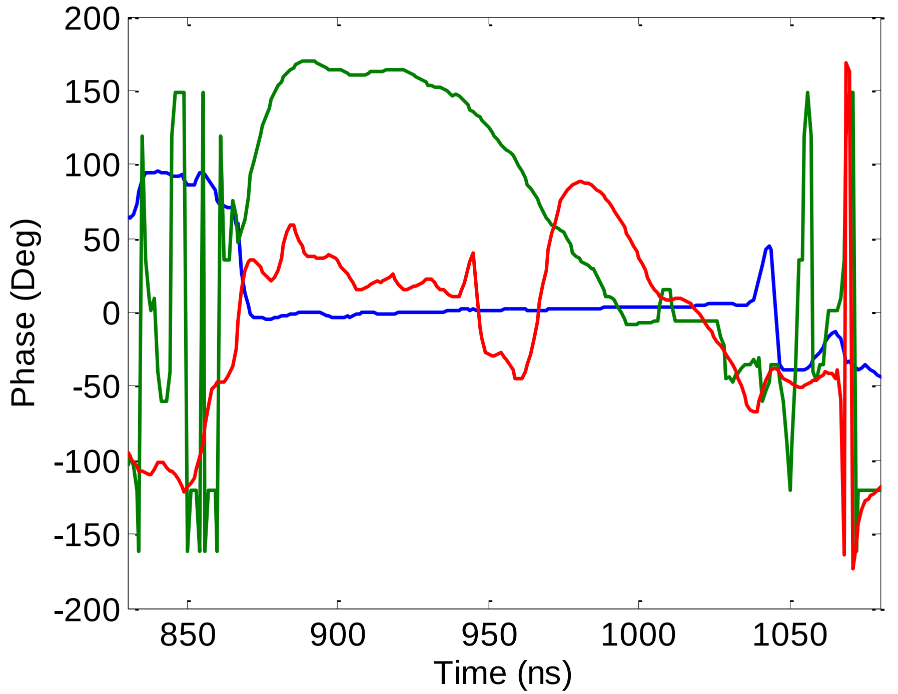

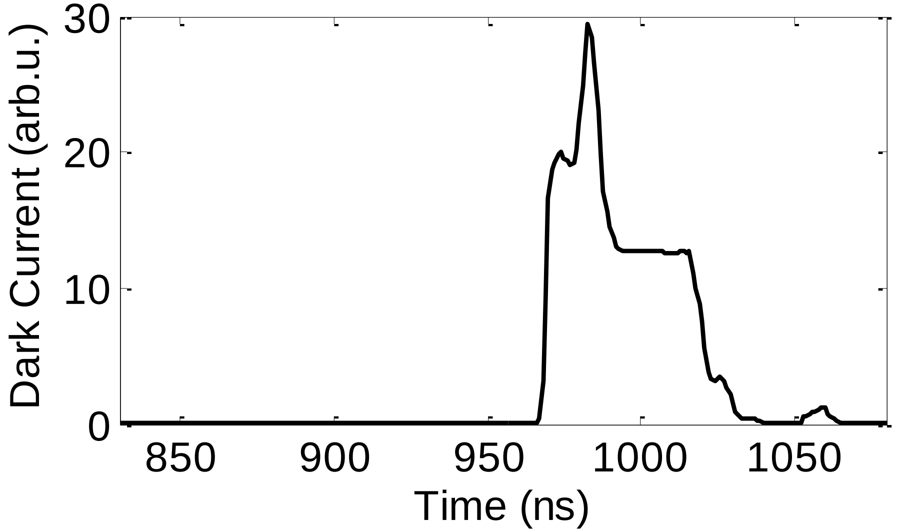

Blue – Input Forward, Green – Output Forward, Red – Input Reflected, Black – dark current.

F. Wang, SLAC
Test of TD18 structure

High Power Operation History

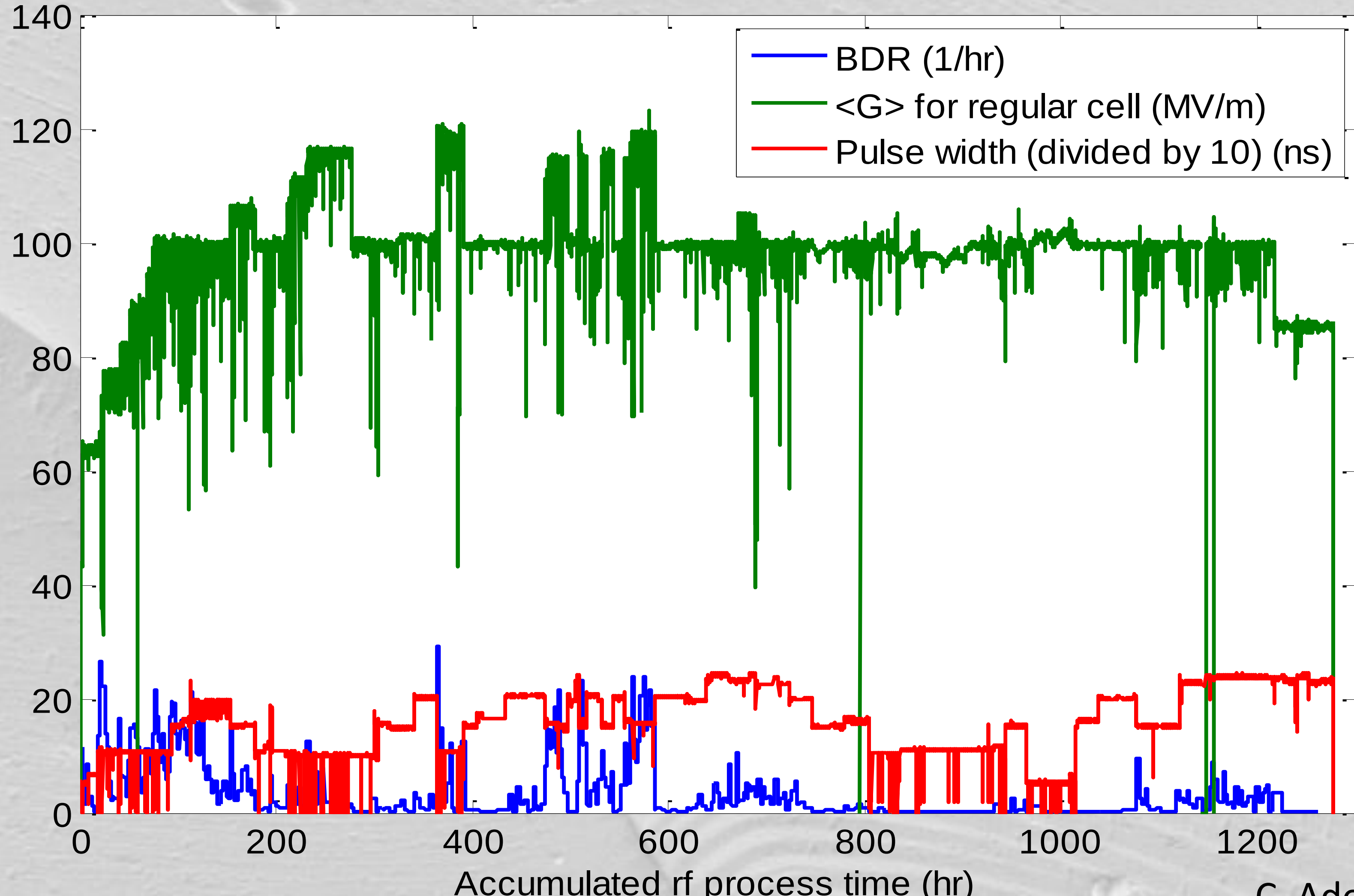

Final Run at 230 ns: 94 hrs at 100 MV/m w BDR = 7.6e-5

60 hrs at 85 MV/m w BDR = 2.4e-6

C. Adolphsen
F. Wang
SLAC

TD18

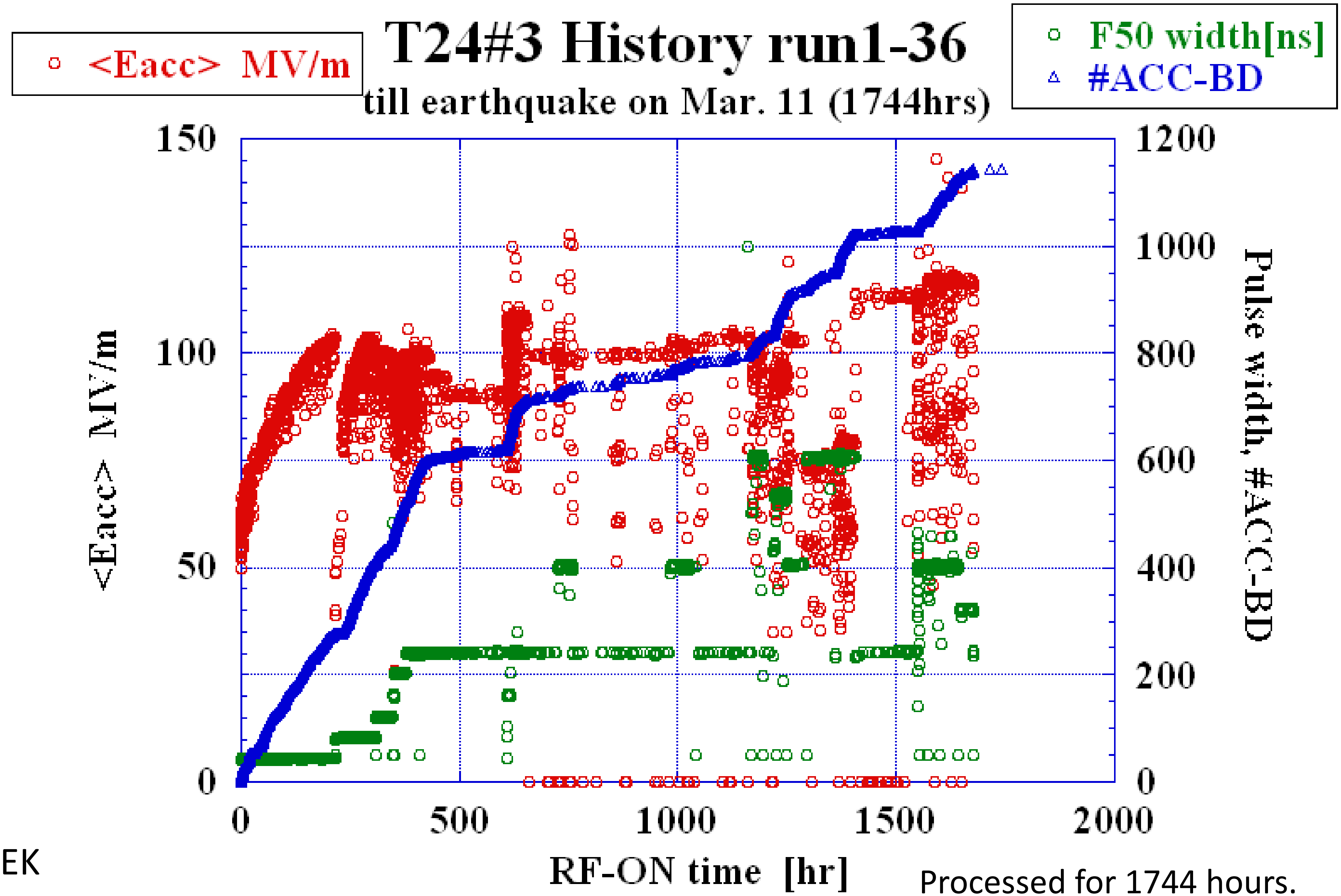

KEK

Processed for 1744 hours.

Breakdown Distribution for T24_SLAC_Disk1 of Last 50 Hours

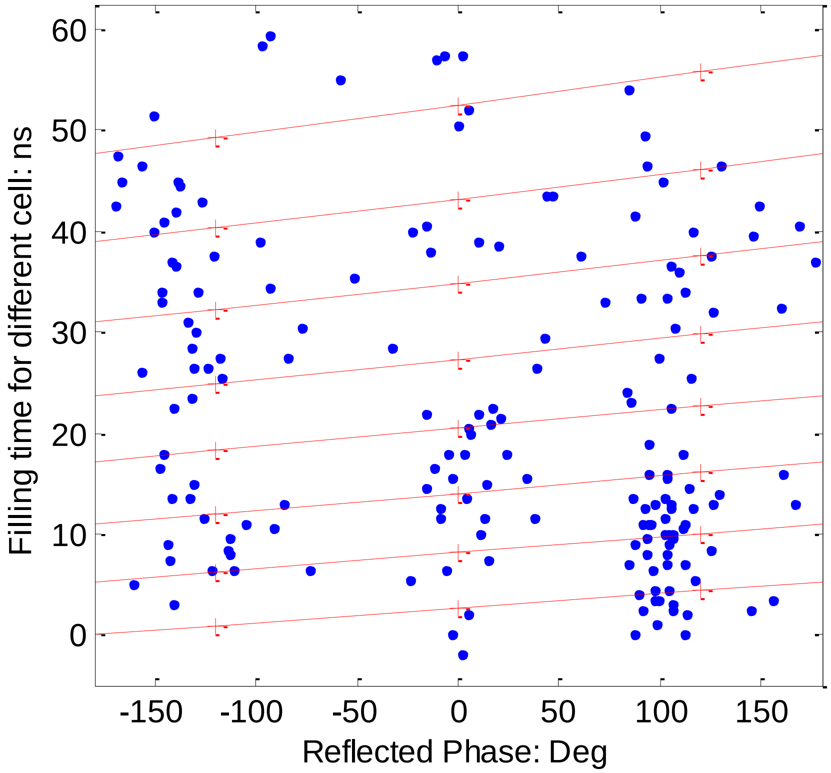

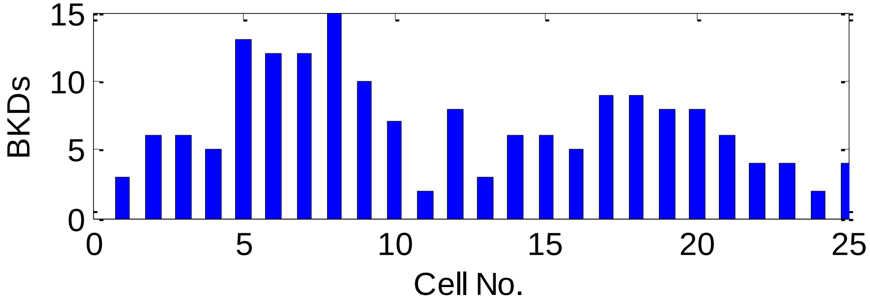

Relevant data points of BDR vs Eacc

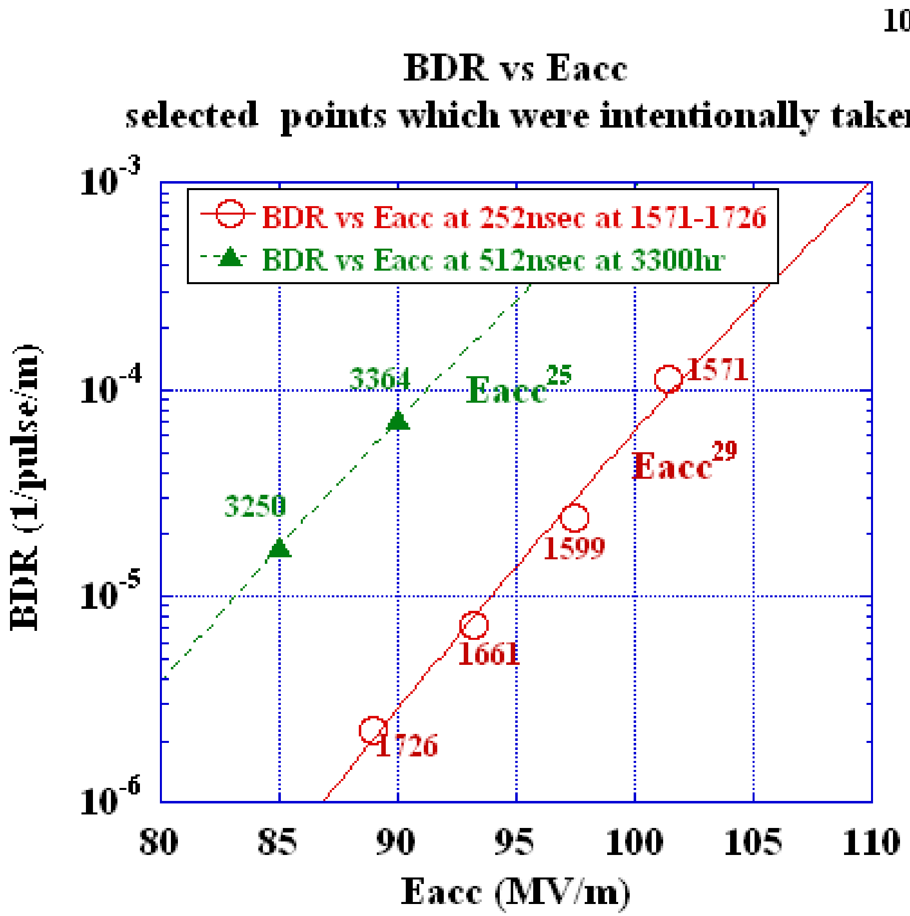

TD18

Steep rise as Eacc, 10 times per 10 MV/m, less steep than T18

TD18_#2 BDR versus width

at 100MV/m around 2800hr and at 90MV/m around 3500hr

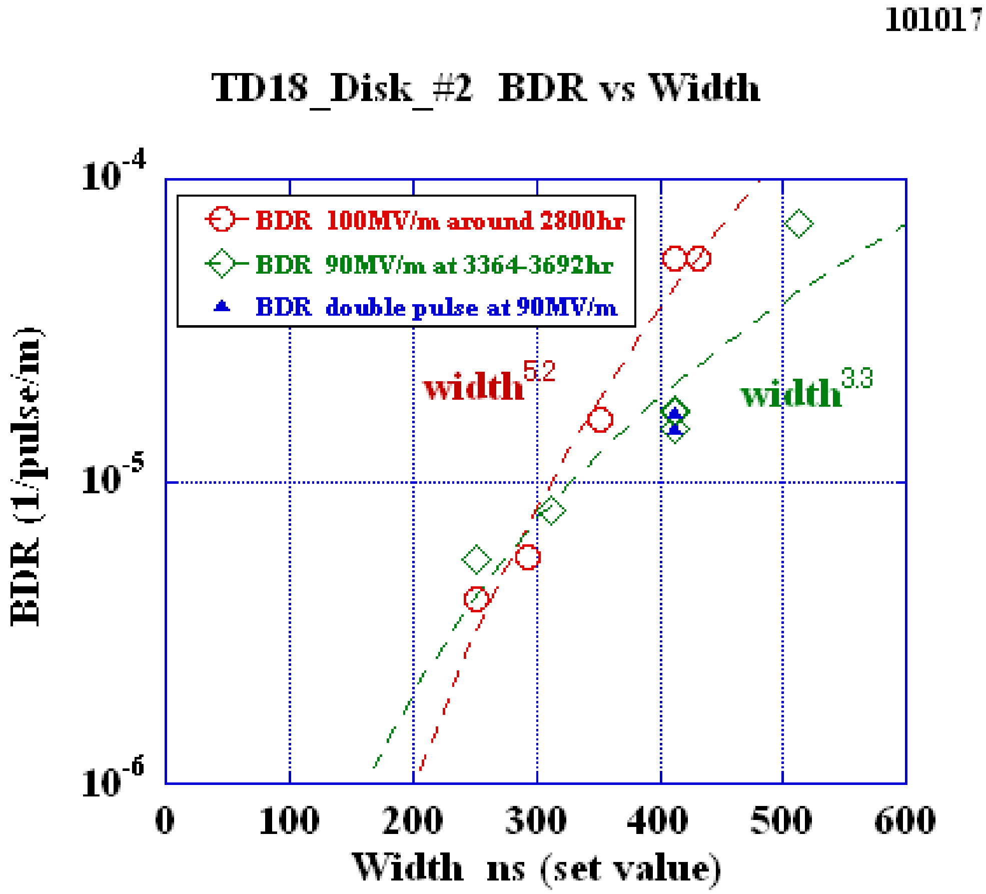

TD18

Similar dependence at 90 and 100 if take usual single pulse?

Summary on gradient scaling

For a fixed pulse length

$$BDR \sim E_a^{30}$$

For a fixed BDR

$$E_a \cdot t_p^{1/6} = const$$

$$\frac{E_a^{30} \cdot t_p^5}{BDR} = const$$

- In **a** Cu structure, ultimate gradient E_a can be scaled to certain BDR and pulse length using above power law. It has been used in the following analysis of the data.
- The aim of this analysis is to find a field quantity X which is geometry independent and can be scaled among **all** Cu structures.

T24#3
BDR evolution at 252ns normalized 100MV/m

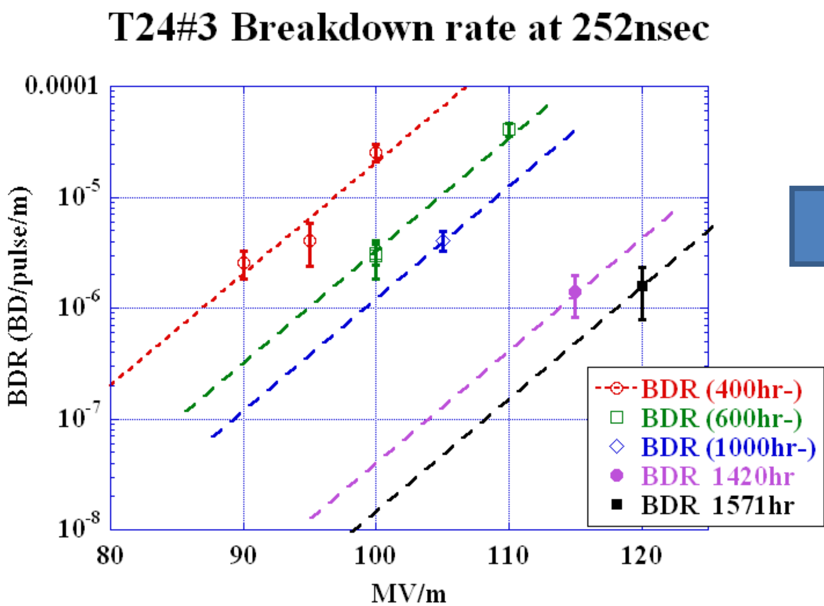

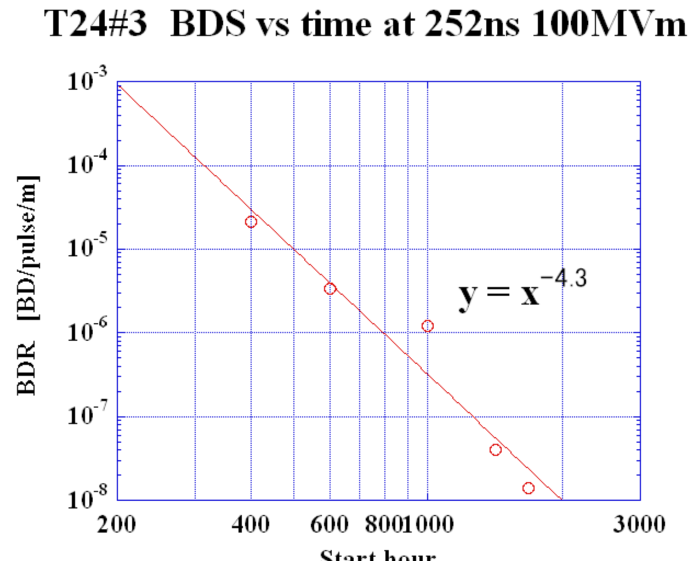

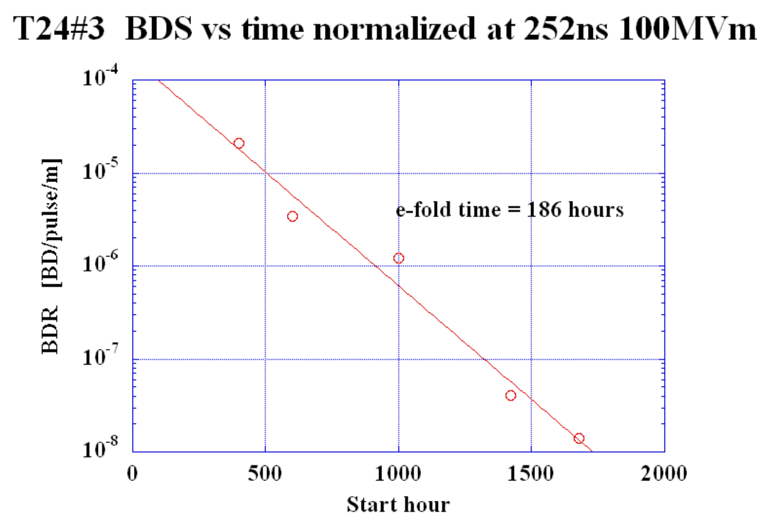

Assuming the same exponential slope as that at 400hr

We understand the BDR has been kept decreasing.

From T. Higo

Breakdown sequence statistics

Both sets of measurements were made on TD18s

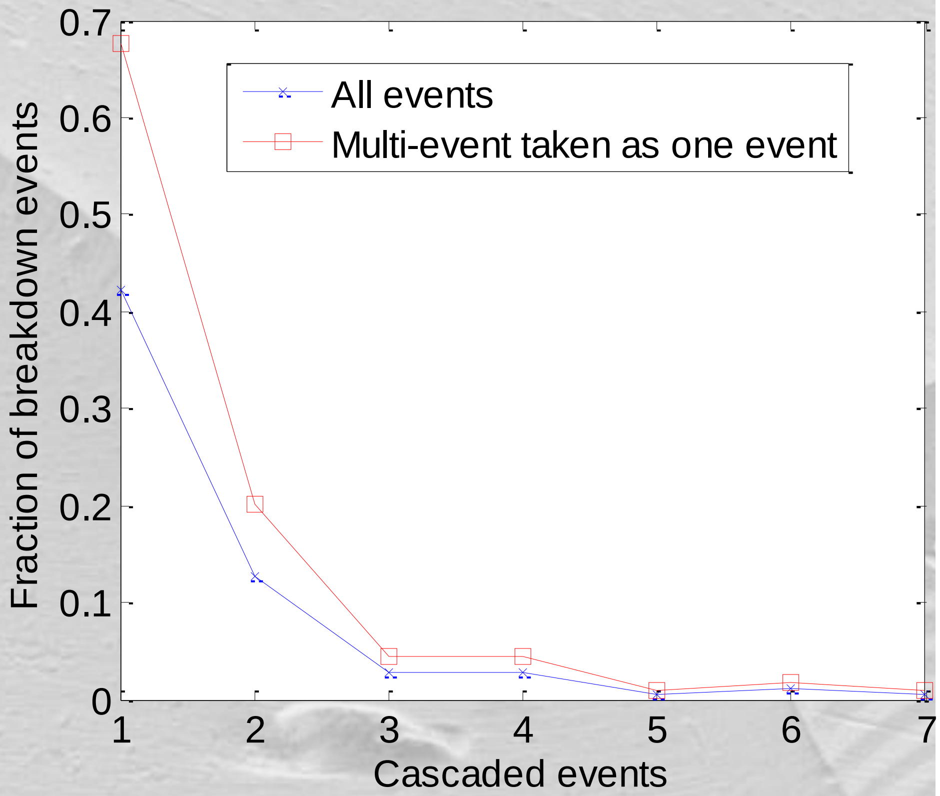

SLAC

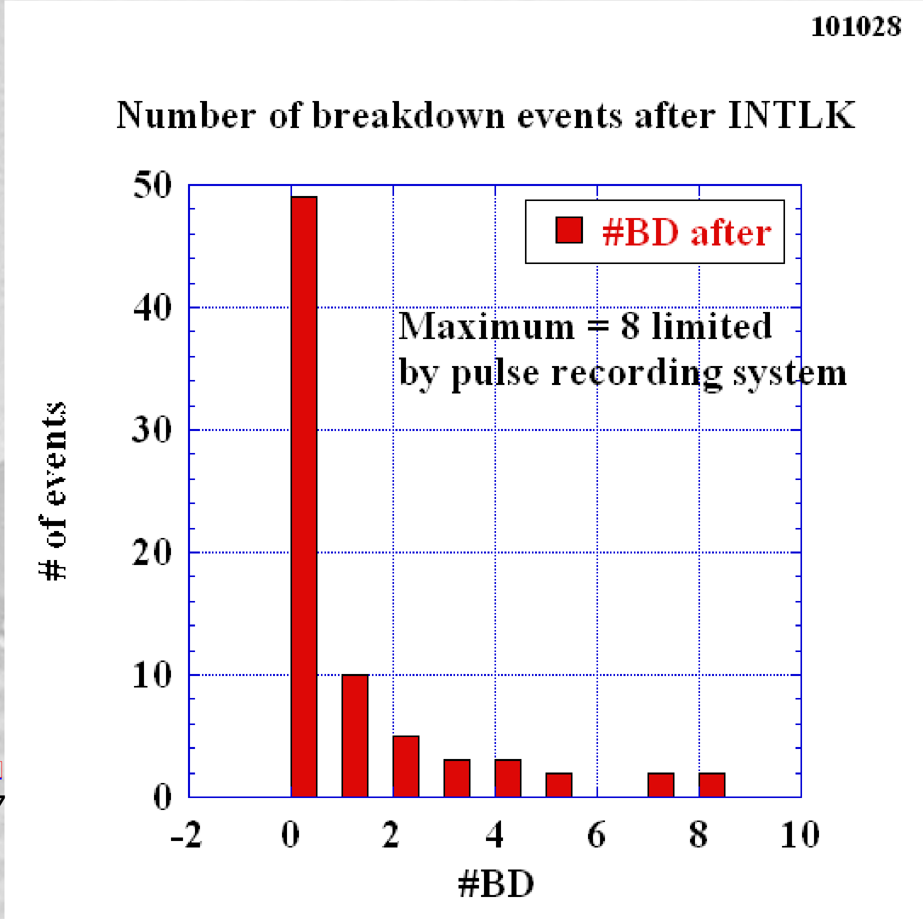

KEK

This kind of data is essential for determining rf hardware – on/off/ramp? – and establishing credible operational scenarios.

18 series breakdown rate distributions

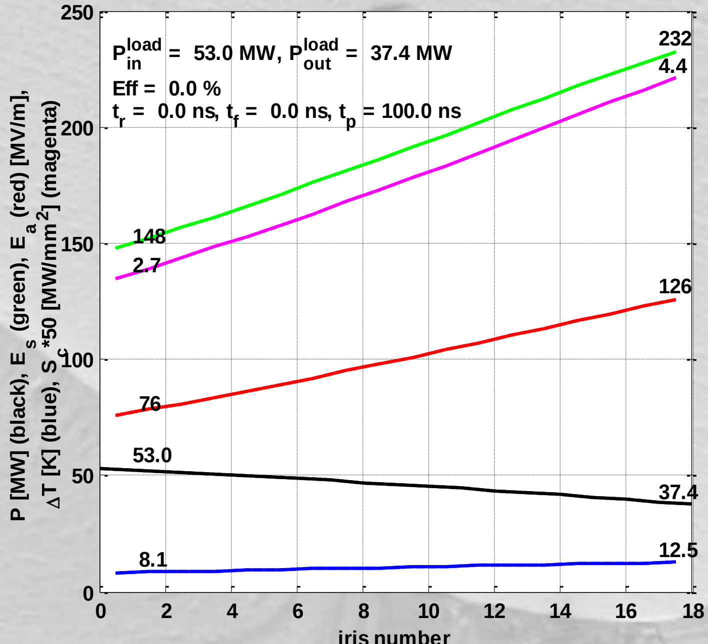

T18

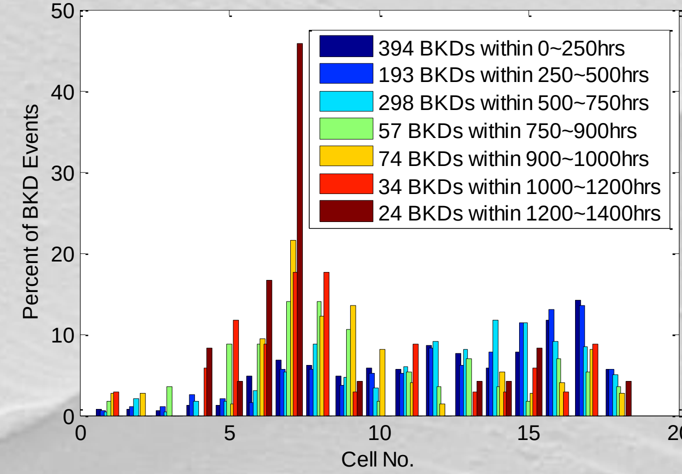

SLAC

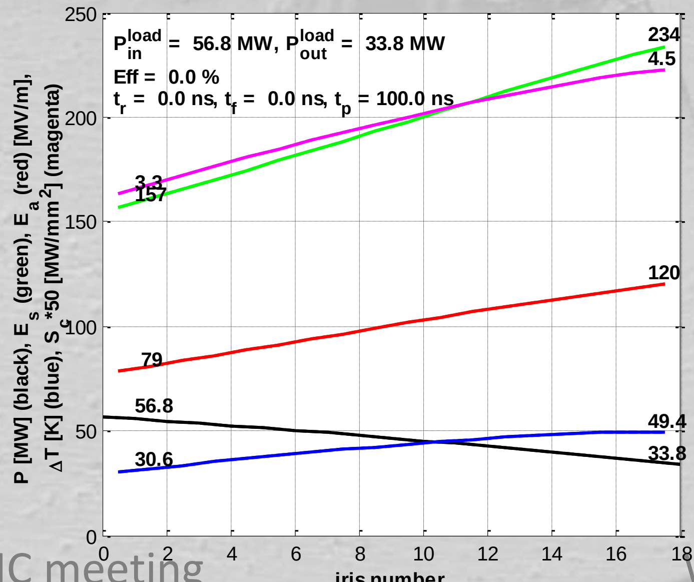

TD18

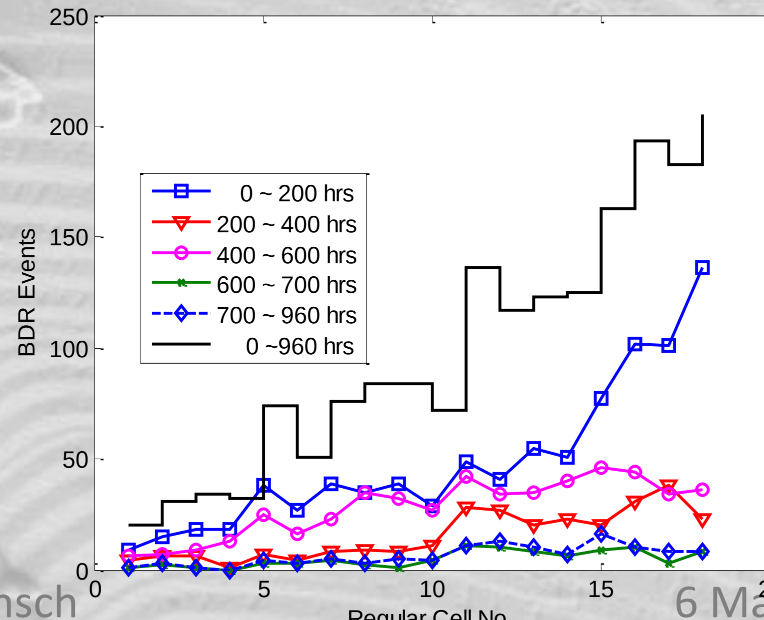

T24 breakdown location distributions

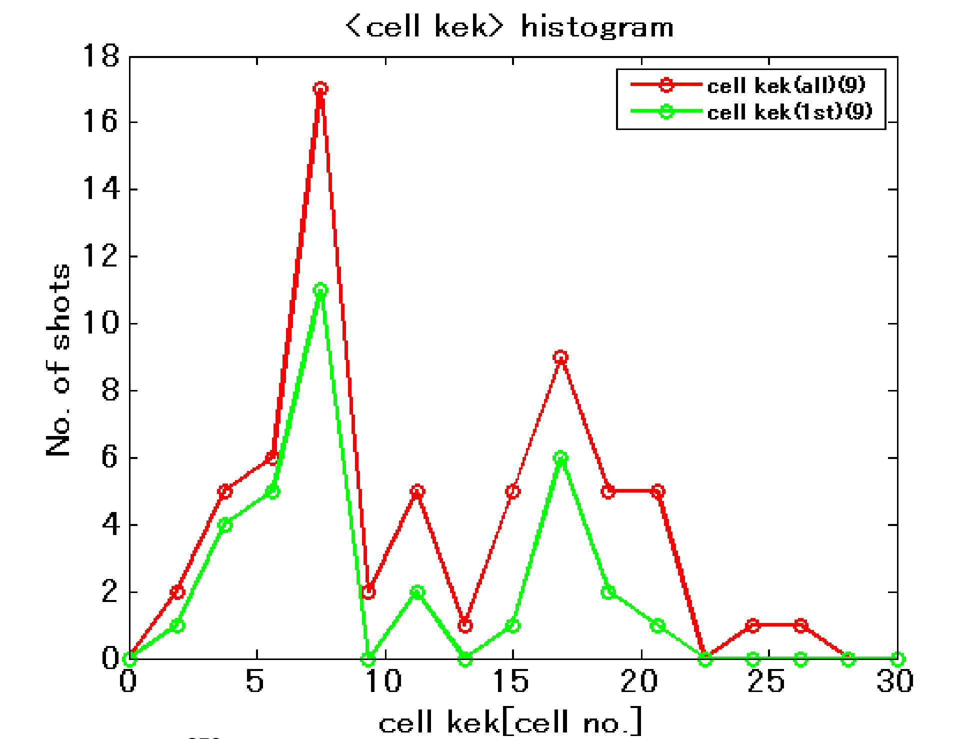

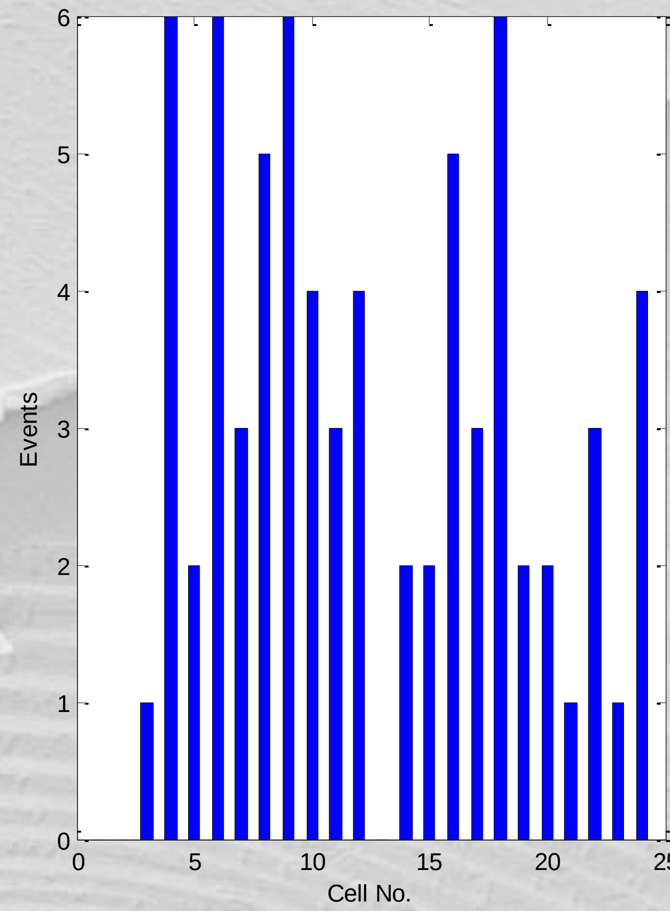

SLAC

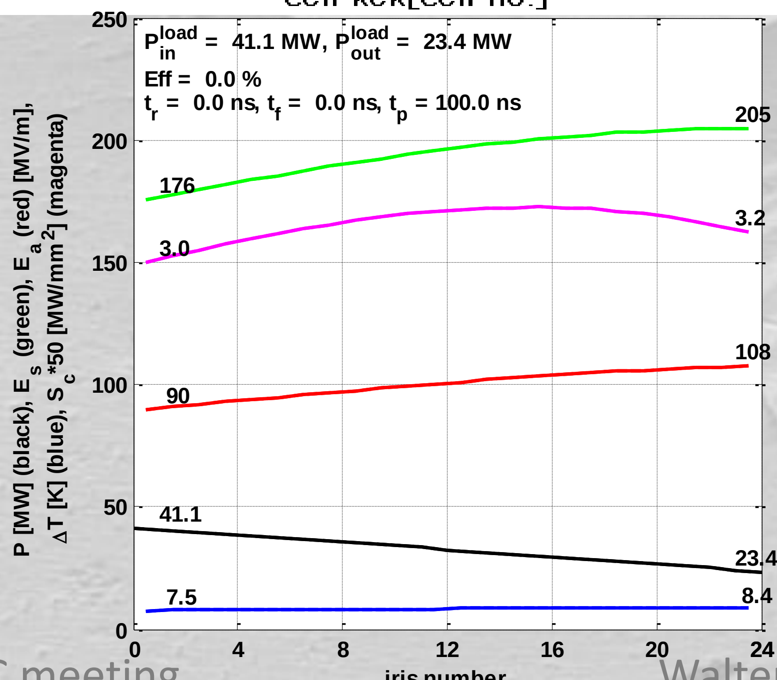

Accelerating gradient test status: 4-9-2012

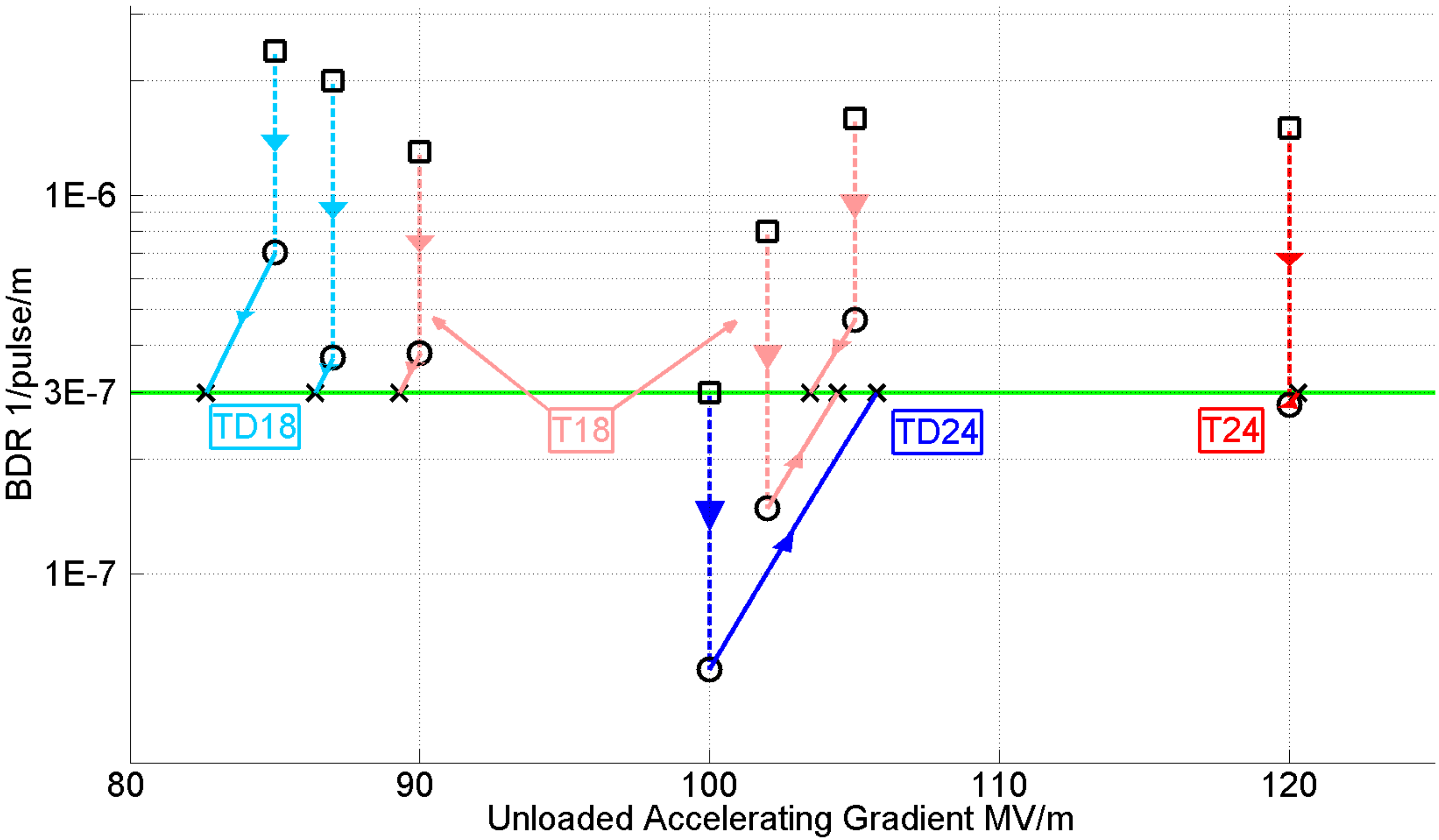

Quantifying geometrical dependence of high-power performance

Importance of geometric dependence - motivation

As you have seen in other presentations, there is a strong interplay between the rf design of accelerating structures and the overall performance of the collider.

One of the strongest dependencies is emittance growth as function of the average iris aperture which acts through transverse wakefields.

The iris aperture also influences required peak power and efficiency through its effect on group velocity.

But crucially the iris aperture has an extremely strong influence on achievable accelerating gradient.

Very generally, we expect that the gradient of an rf structure should be calculable from its geometry if material and preparation are specified.

The big questions

Where does such a geometrical dependency come from?

Can we quantify the dependence of achievable accelerating gradient on the geometry?

Trying to understand, derive and quantify geometrical dependence has been a significant effort because an essential element of the overall design and optimization of the collider.

The basic approach

The basic element is to express our high-power limits as a function of the unperturbed fields inside our structures – like the electric field limit in dc spark.

So first we are going to make sure that we have a feel for how those fields vary as a function of geometry.

We use a specific example of iris variation for a fixed phase advance in a travelling wave structure.

Field distribution

Electric field (V/m)

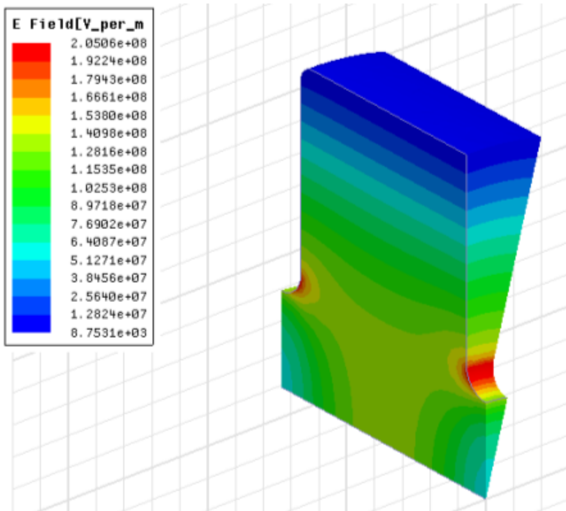

Magnetic field (A/m)

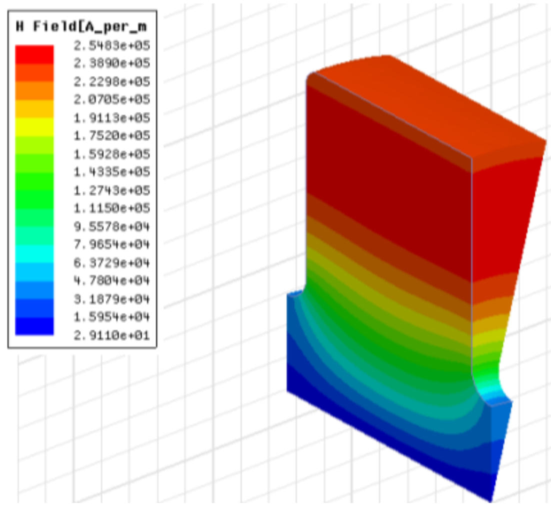

Poynting vector (W/m^2)

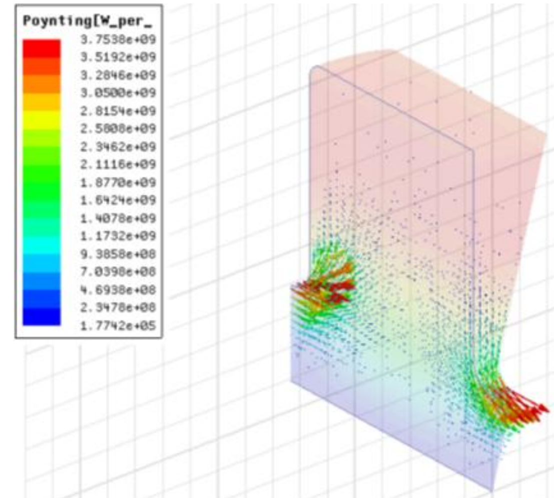

- Simulation in HFSS12
- Field values are normalized to accelerating gradient, E_{acc}=100MV/m
- Frequency: 11.424GHz
- Phase advance per cell: 120 degree
- *Iris radius*: 3mm
- v_g /c= 1.35%

Parameters v.s. iris

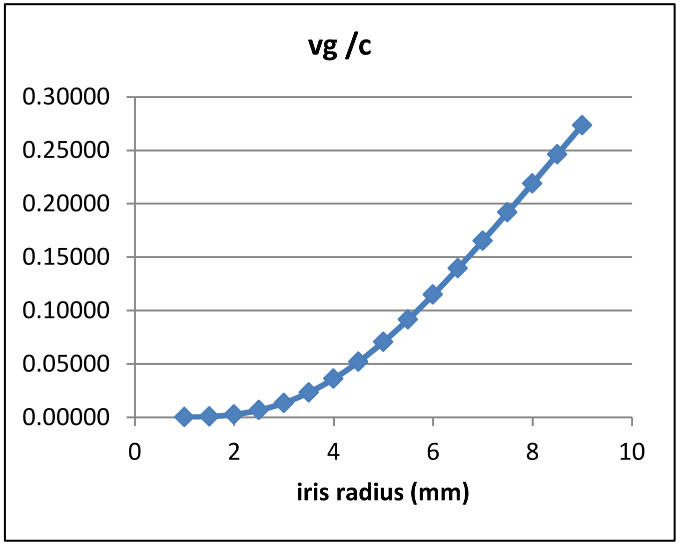

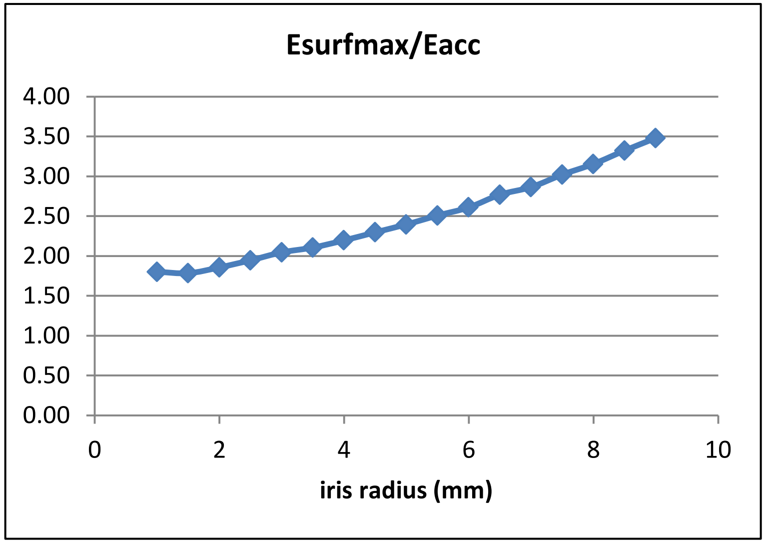

Simulation in HFSS12
Iris thickness: 1.66mm
Frequency: 11.424GHz
Phase _adv/cell: 120 degree

$$R/Q = V^2_{acc}/(\omega U)$$

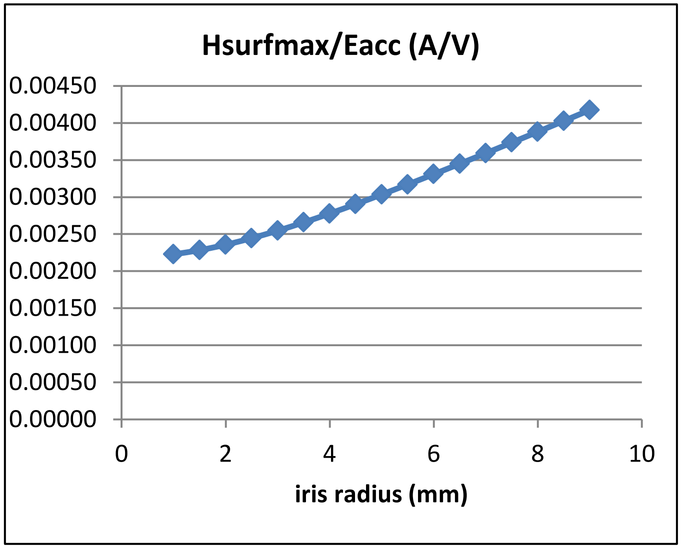

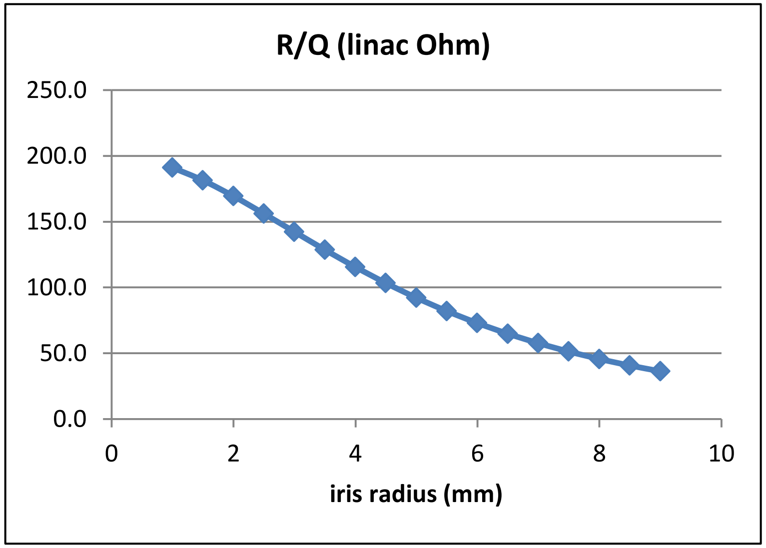

Overview of how different types of structures behave – from accelerating structures to PETS

Achieving high gradients has been a high profile concern for CLIC and NLC/JLC since roughly 2000. Here are the target specifications we have had:

	frequency [GHz]	Average loaded gradient [MV/m]	Input (output for PETS) power [MW]	Full pulse length [ns]
NLC/JLC	11.424	50	55	400
CLIC pre-2007				
Accelerating	29.928	150	150	70
PETS	29.985	-5.7	642	70
CLIC post 2007				
Accelerating	11.994	100	64	240
PETS	11.994	-6.3	136	240

Trying to achieve these specifications has resulted in the test of many structures of diverse rf design over the years.

The preparation and testing conditions of the test structures which were built were not always the same – these processes also evolved over the period the structures were being developed.

But the wide variety of structure geometries were tested under reasonably similar conditions.

So we have used this unique set of data to try to understand and then quantify the geometrical dependency of gradient.

High-power design criteria

The functions which, along with surface electric field and magnetic field (pulsed surface heating), give the high-gradient performance of the structures are:

$$\frac{P}{\lambda C} = \text{const}$$

global power flow

$$S_c = \mathrm{Re}(\mathbf{S}) + 6\,\mathrm{Im}(\mathbf{S})$$

local complex power flow

These are now standard design criteria used throughout the CLIC structure program. We are actively pursuing checking their validity over a wider range of parameters and putting them on a more solid footing.

Maximum surface electric and magnetic fields

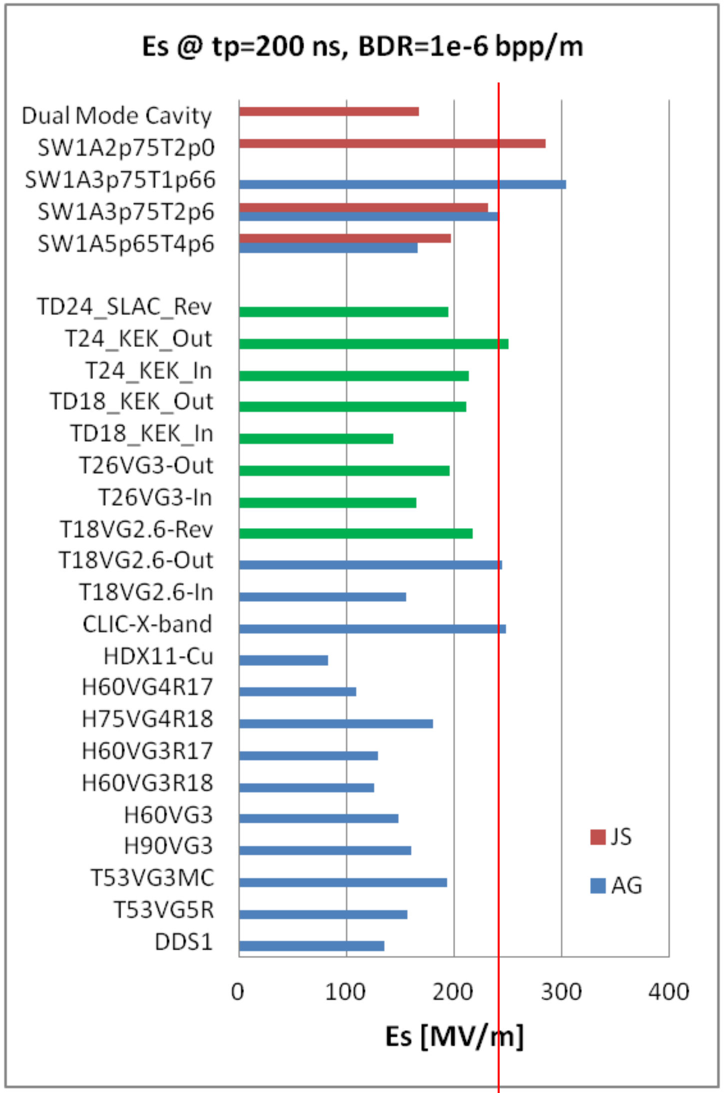

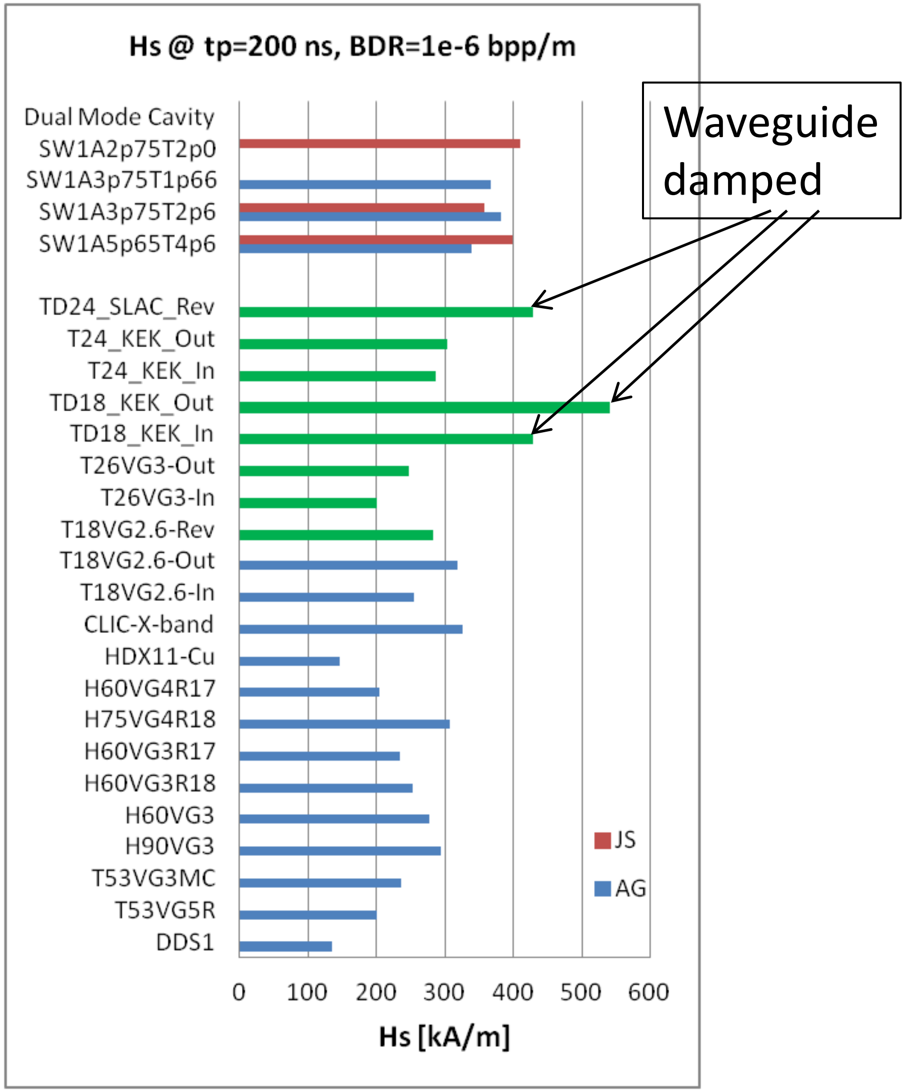

Es = 250 MV/m or higher has been achieved in several cases: very low or zero group velocity

Power flow related quantities: Sc and P/C

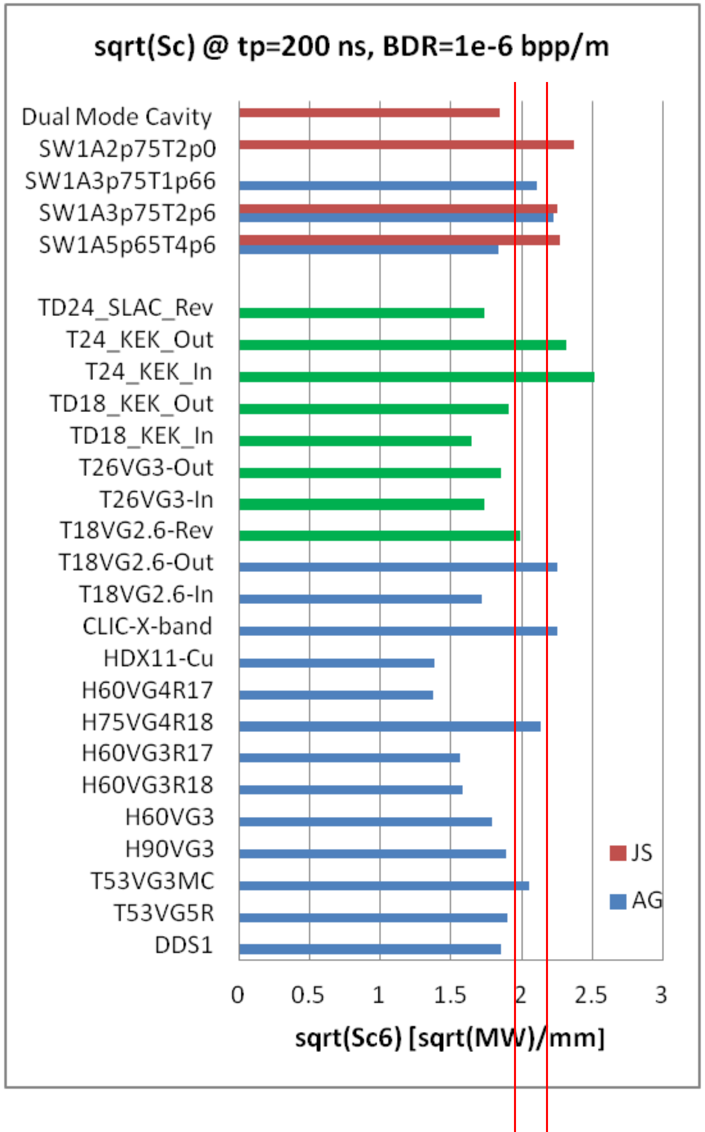

Sc = 4 - 5 MW/mm^2

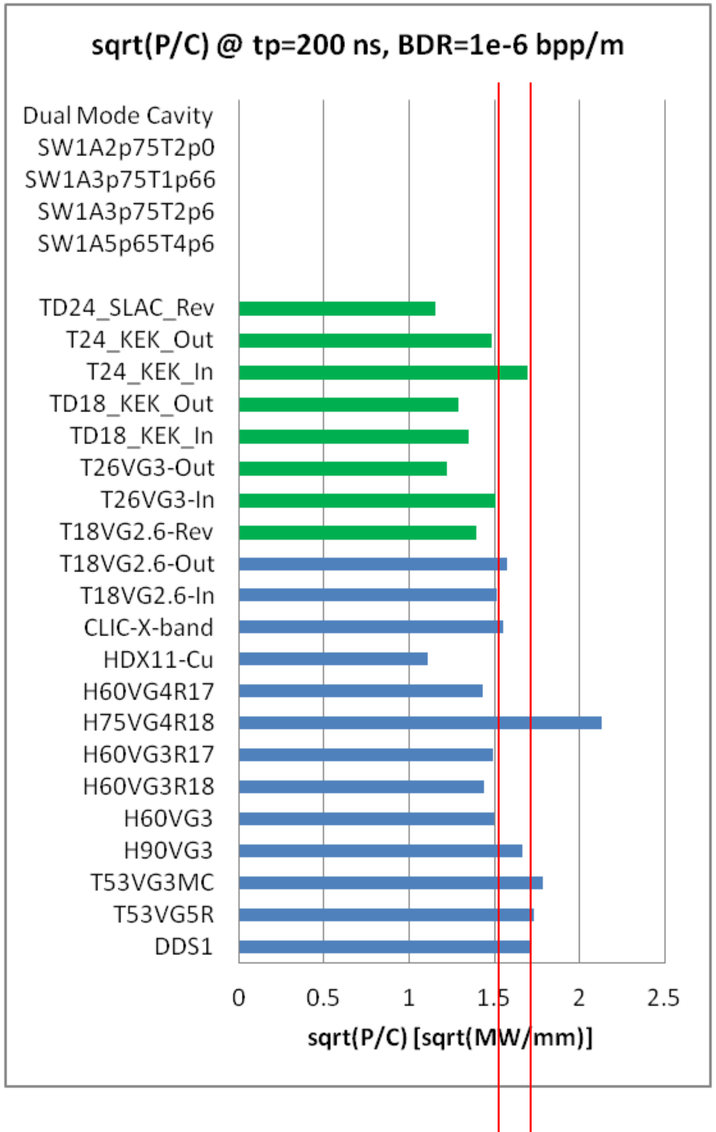

P/C = 2.3 – 2.9 MW/mm

Optimization procedure

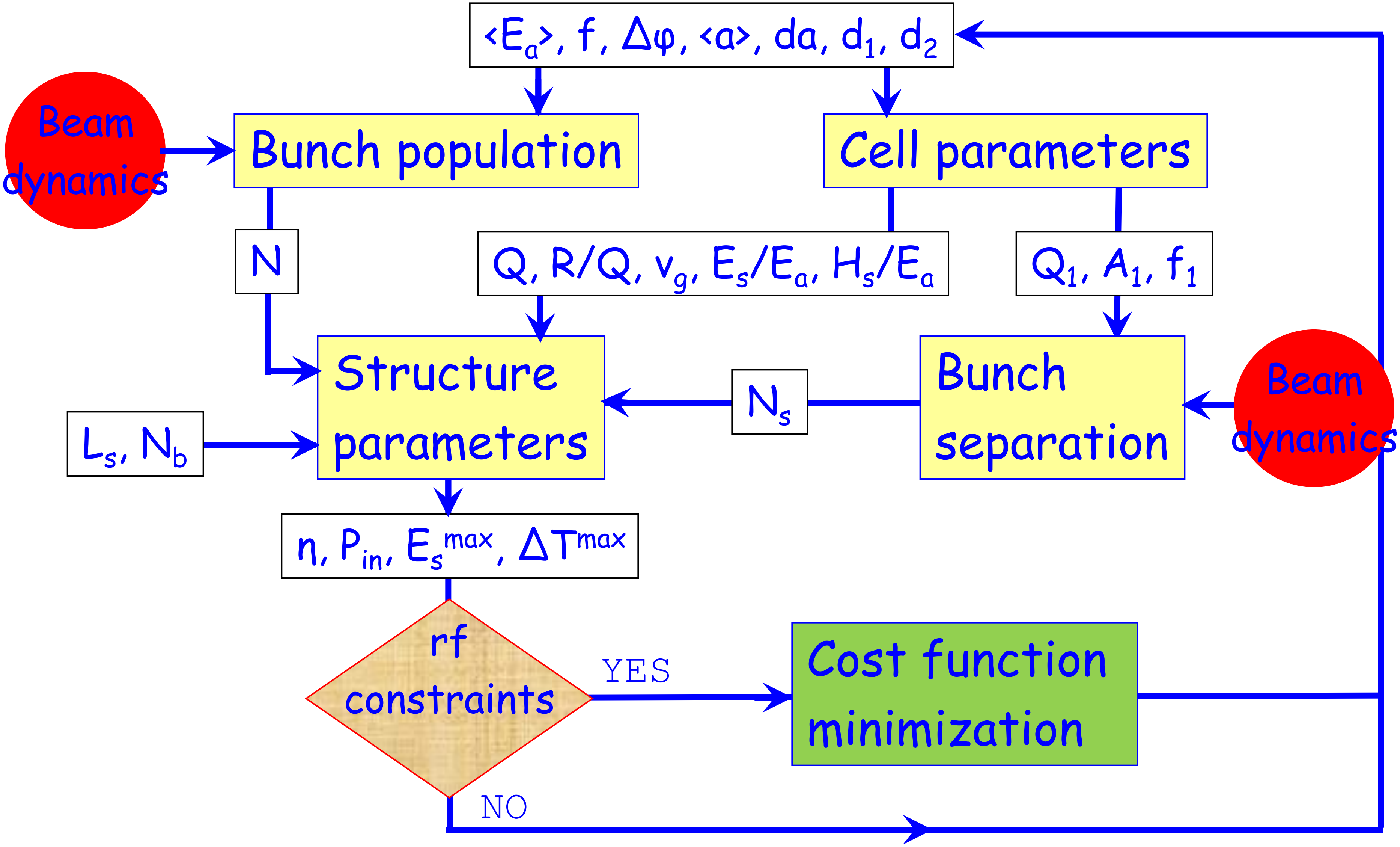

Simplified Diagram

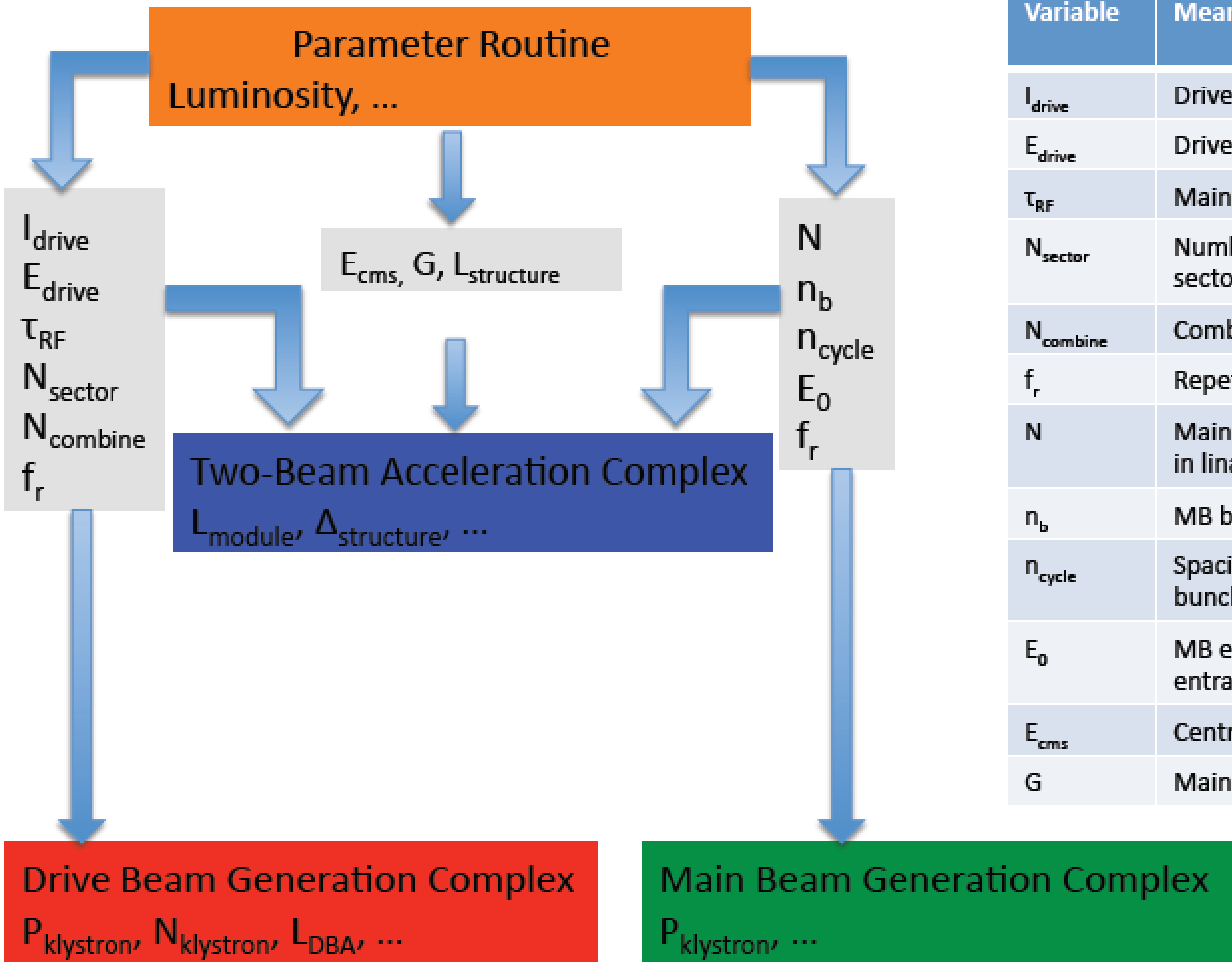

Variable	Meaning	Current value
I_{drive}	Drive beam current	101A
E_{drive}	Drive beam energy	2.37GeV
τ_{RF}	Main lianc RF pulse length	244ns
N_{sector}	Number of drive beam sectors per linac	4
$N_{combine}$	Combination number	24
f_r	Repetition rate	50Hz
N	Main beam bunch charge in linac	3.72e9
n_b	MB bunches per pulse	312
n_{cycle}	Spacing between MB bunches	6 cycles
E_0	MB energy at linac entrance	9GeV
E_{cms}	Centre-of-mass energy	500GeV
G	Main linac gradient	100MV/m

D. Schulte

Breakdown!

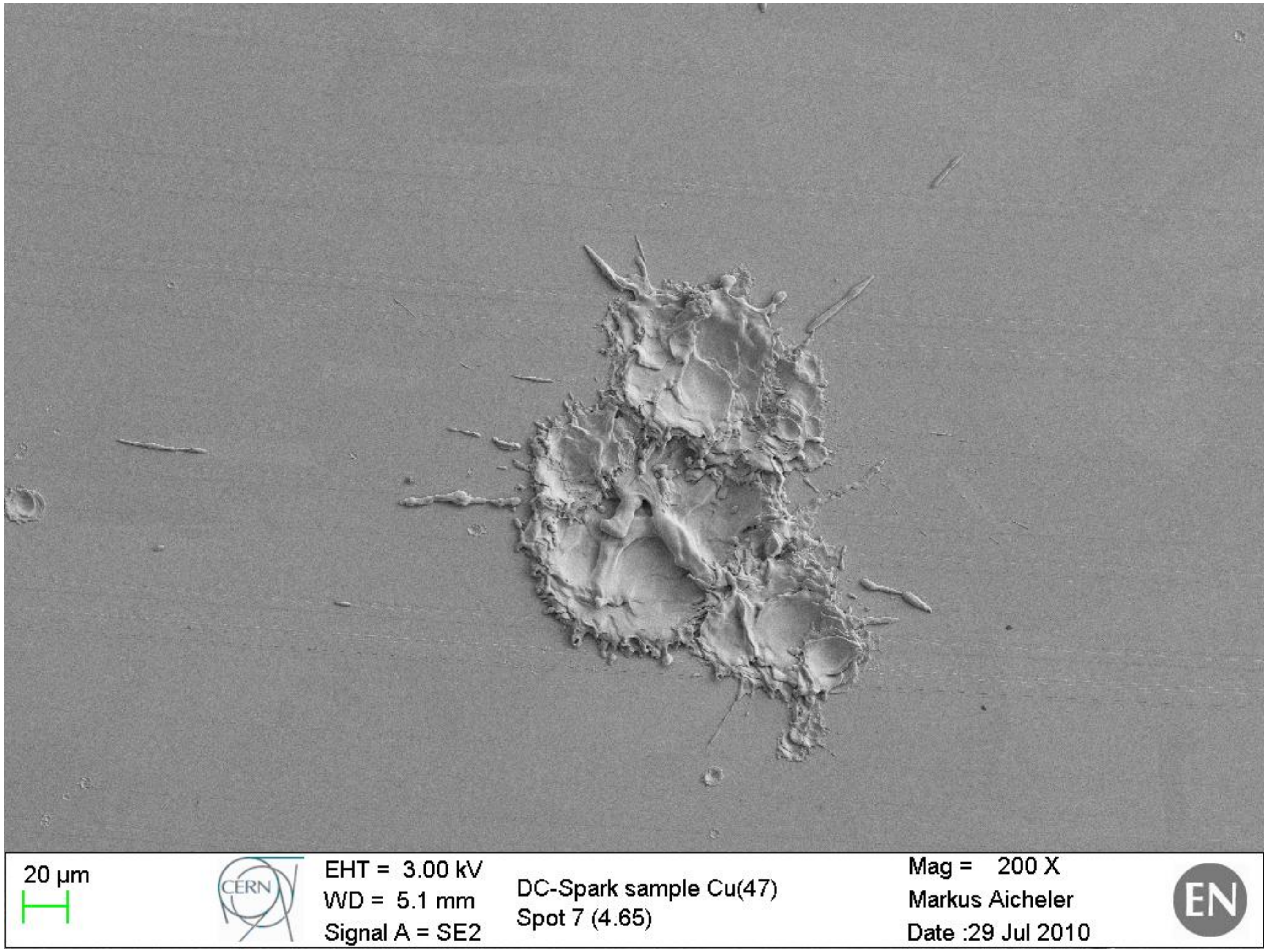

From pA to kA and from Angstroms to 100s of μm to mms.

The multiscale breakdown process

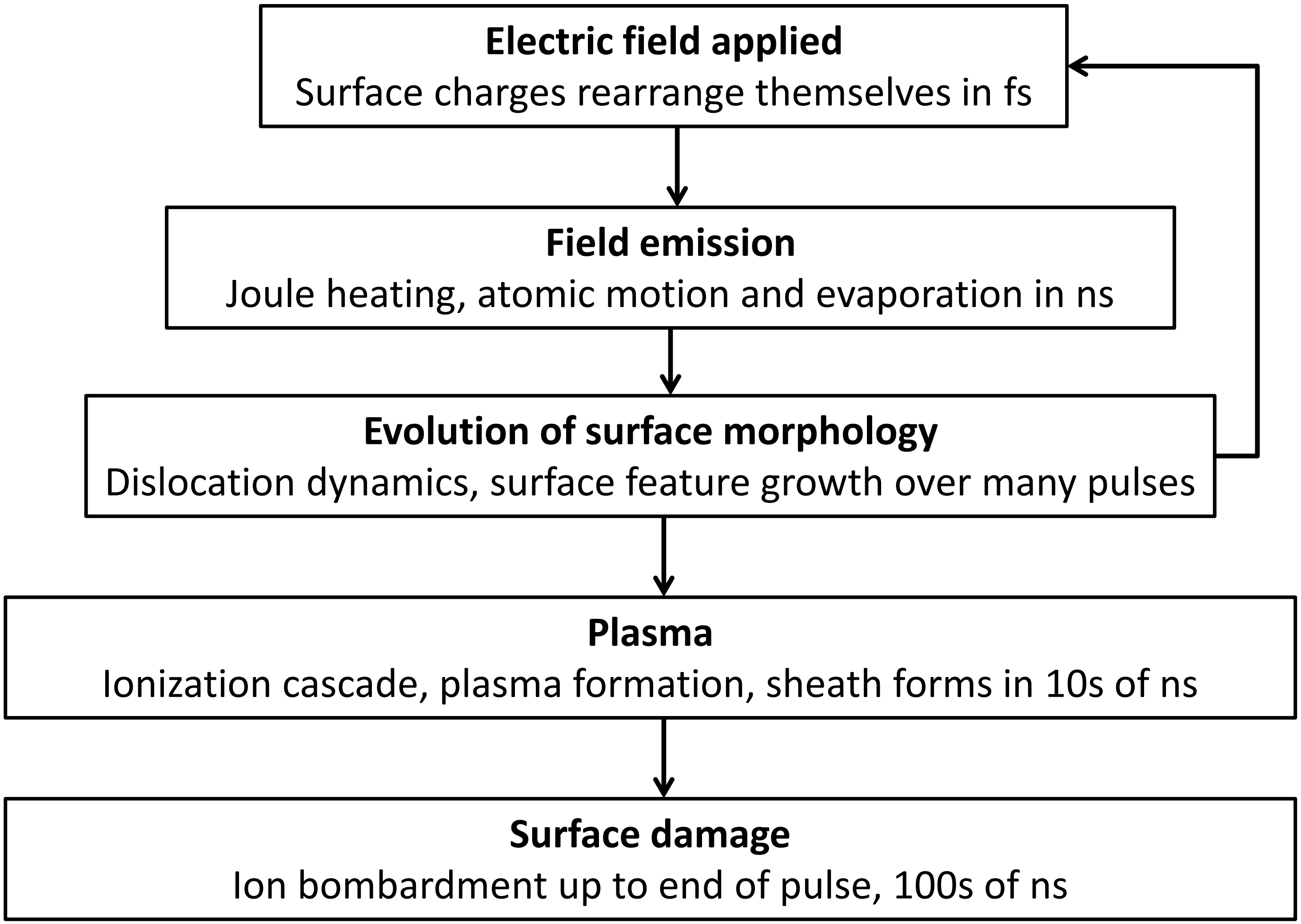

based on a slide by Flyura Djurabekova

The surface potential used for solving the Fowler-Nordheim equation

$$V(z) = \begin{cases} -W_a & \text{for } z<0 \\ -eEz - e^2/4z & \text{for } z>0 \end{cases}$$

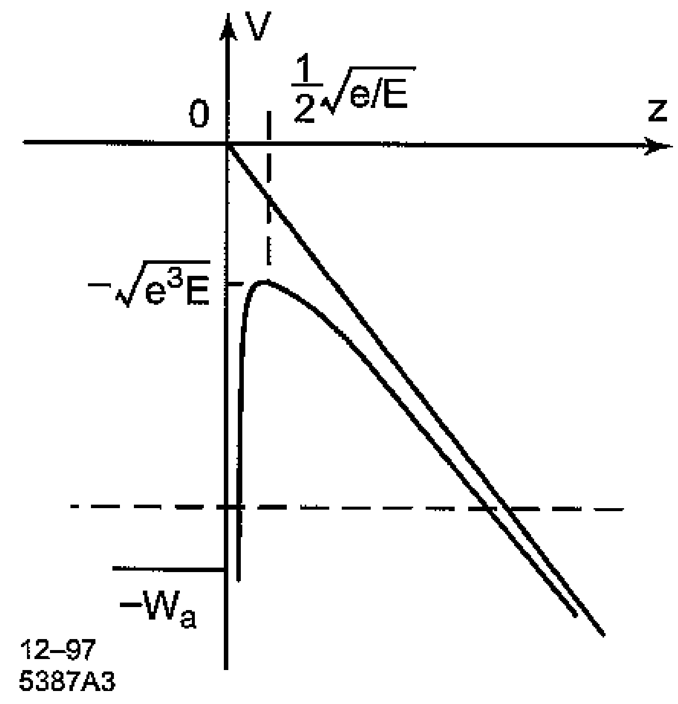

The Fowler-Nordheim equation (approximate, practical form)

$$I = A_e \frac{1.54\times10^6 \beta^2 E^2}{\varphi} e^{10.41\varphi^{-1/2}} \times e^{-6.53\times10^3\times\varphi^{3/2}/\beta E}$$

$$= \xi E^2 e^{-6.53\times10^3 \varphi^{3/2}/\beta E}$$

Units: [I]=A, [E]=MV/m, [A_e]=m^2, [φ]=eV and [β]=dimensionless

Values: φ = 4.5 eV for copper

The Fowler-Nordheim equation
Analyzing real data

$$I = \xi E^2 e^{-\gamma / E}$$

$$\ln\left(\frac{I}{E^2}\right) = \ln(\xi) - \frac{\gamma}{E}$$

$$\beta = \frac{6.53 \times 10^3 \varphi^{3/2}}{\gamma}$$

$$\zeta = A_e \frac{1.54 \cdot 10^6 \beta^2}{\varphi} \exp(10.41 \cdot \varphi^{-1/2})$$

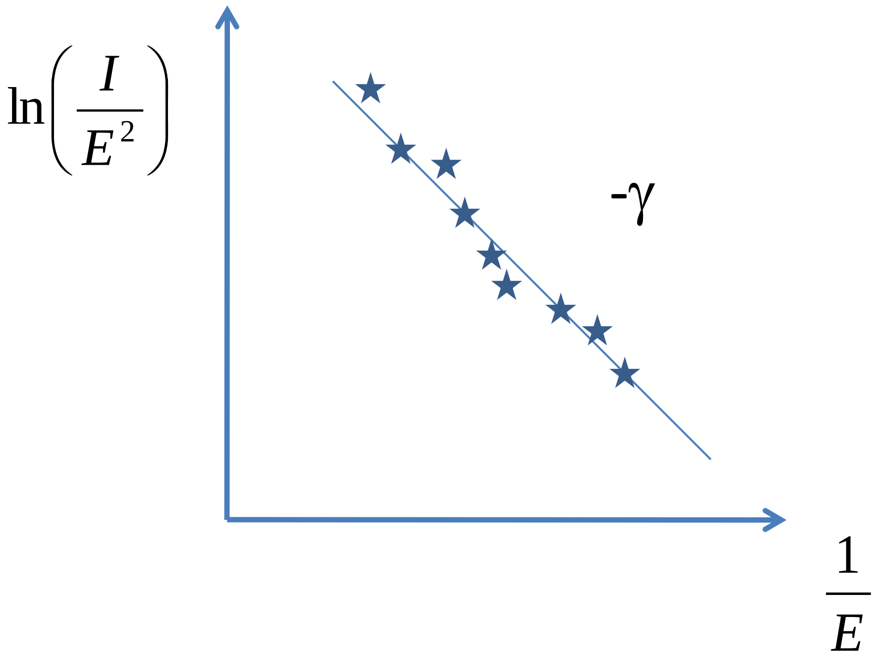

You will have the opportunity to analyze a real set of data tonight for homework!

Effective Fowler-Nordheim Field Emission

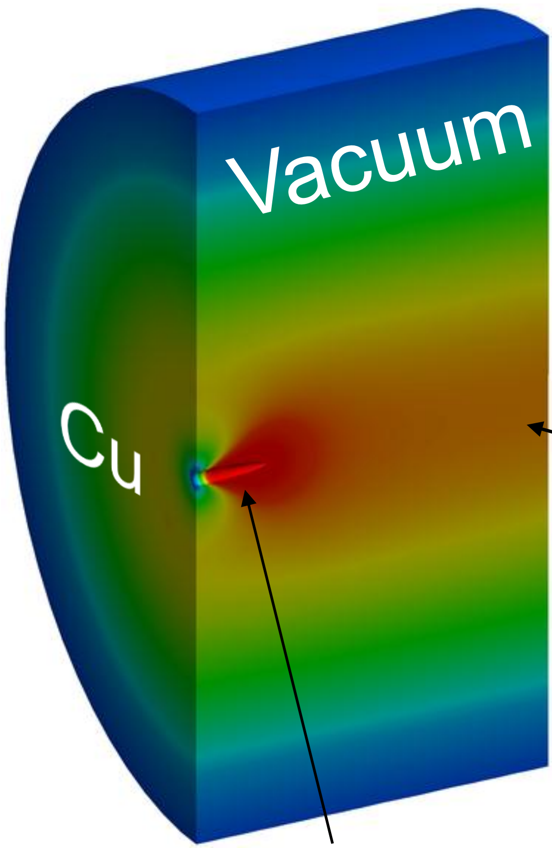

Self-consistent effective FN field emission in RF and space charge fields using Pic3P

RF surface field map computed with Omega3P (then driven at f=12 GHz)

Assumptions:
- 200 MV/m surface fields (E_{acc}=100 MV/m)
- Tip does not change (fixed β=50)
- No transport phenomena
- No heating effects
- Particles emitted without energy spread

Single microscopic Cu tip protruding from surface of RF structure, RF field shown (|E|)

maximum emission current can be limited to simulate "self-healing" of sharp protrusions (realistic?)

Pic3P Field Emitter Space-Charge Modeling

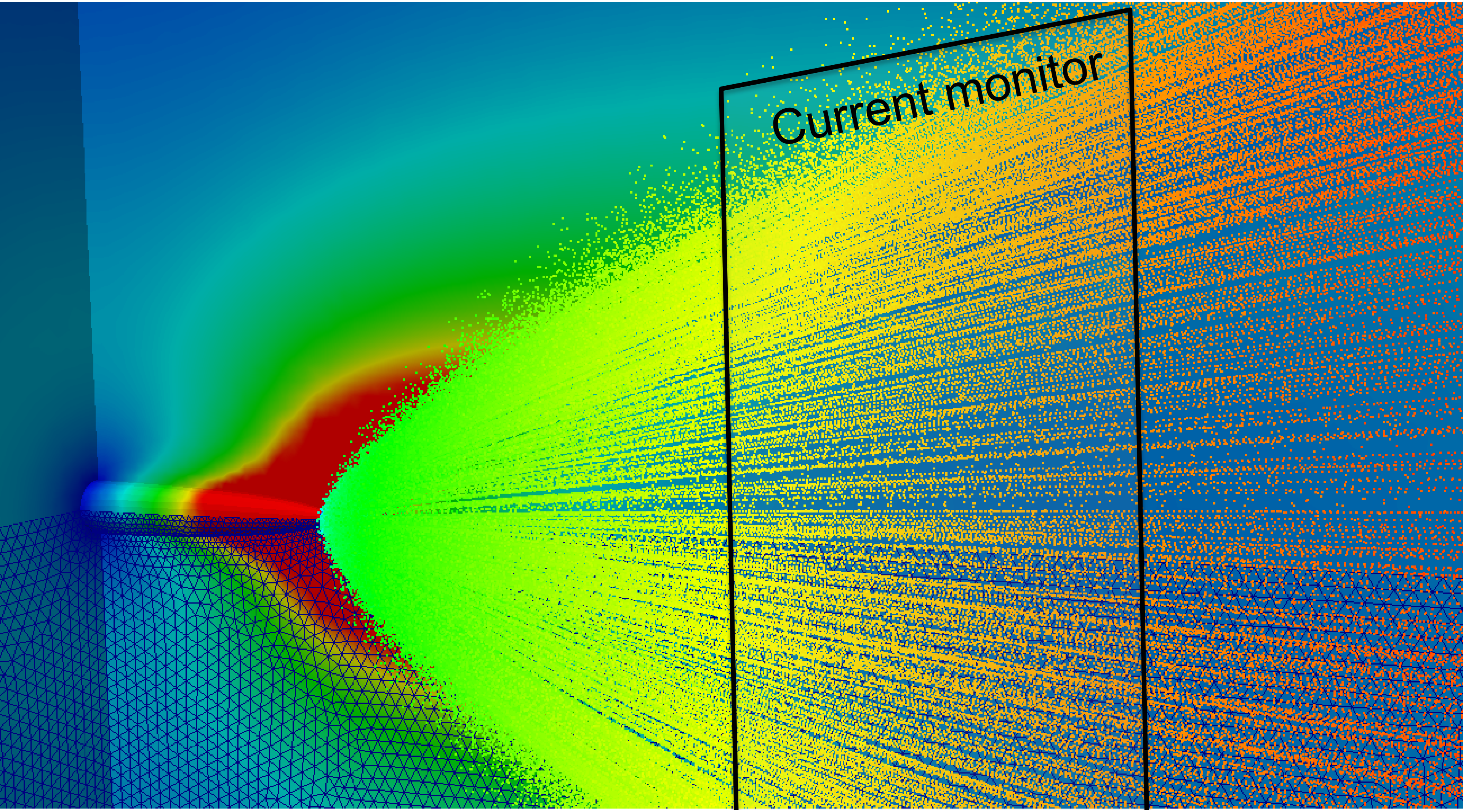

space-charge field |E| in vertical symmetry plane
electrons colored by momentum

Space-Charge Fields (Contours of |E|=const)

(Case 2)

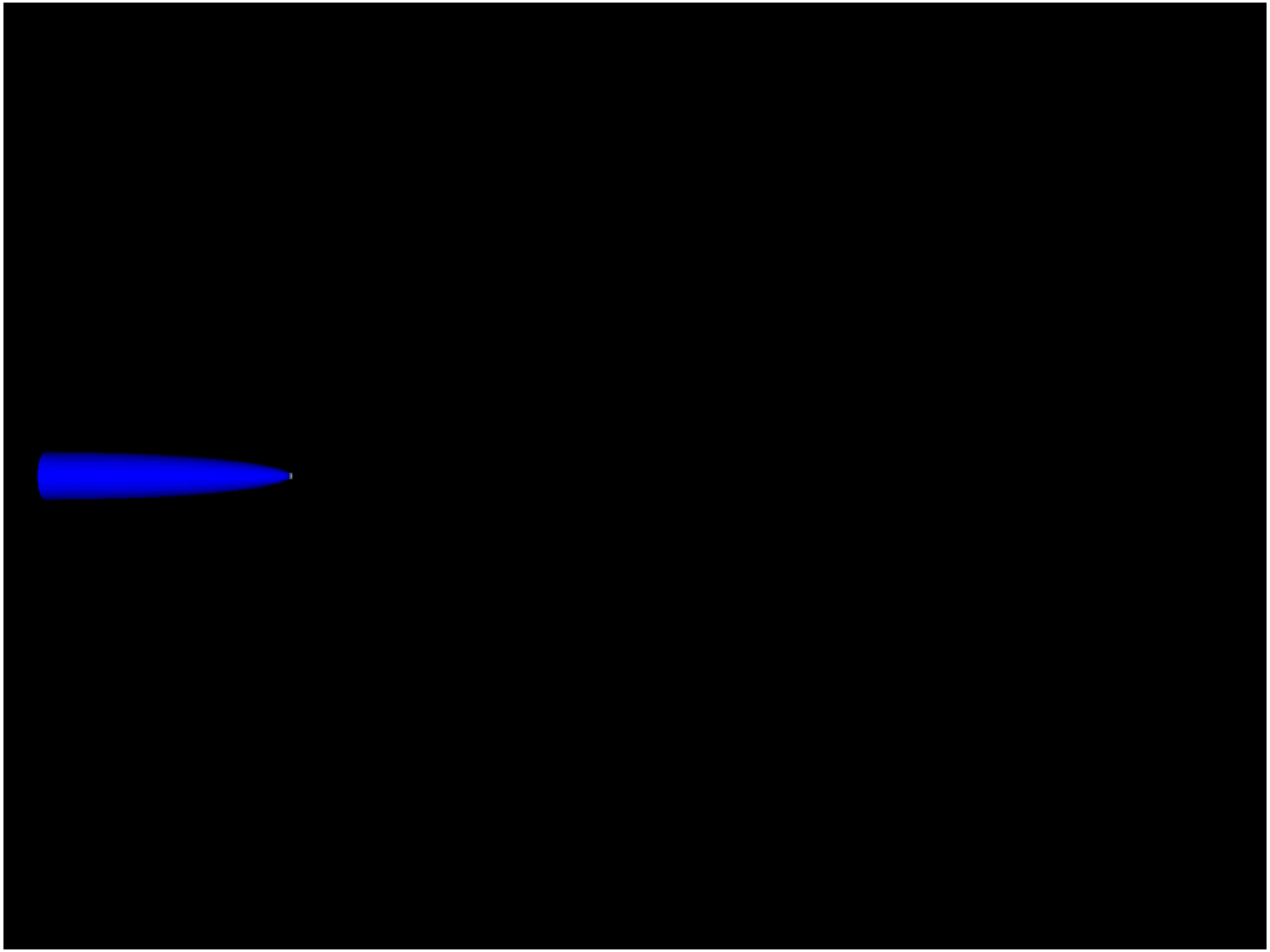

red: |E|>1 MV/m, max: ~2.5 GV/m

Electron emission

Fowler Nordheim Law (RF fields):

$I_{FN}(\beta, \phi_0, A_e, E_0)$

$$\bar{I} = \frac{5.79\times10^{-12}\exp(9.35\varphi_0^{-0.5})A_e(\beta E_0)^{2.5}}{\varphi_0^{1.75}}\exp\left(\frac{-6.53\times10^{9}\varphi_0^{1.5}}{\beta E_0}\right)$$

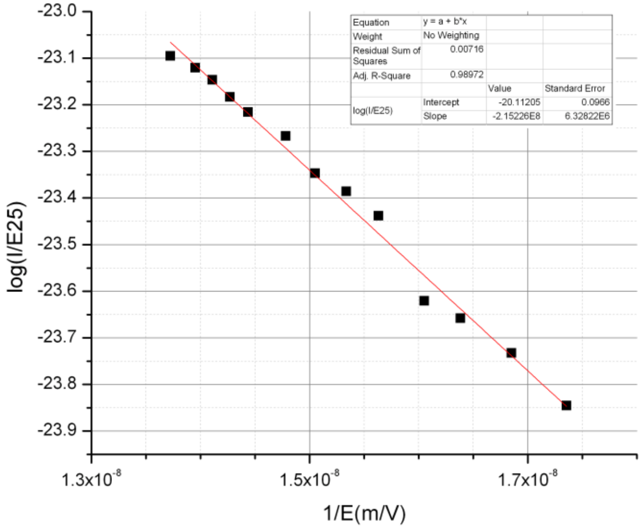

Equation	y = a + b*x		
Weight	No Weighting		
Residual Sum of Squares	0.00716		
Adj. R-Square	0.98972		
		Value	Standard Error
log(I/E25)	Intercept	-20.11205	0.0966
	Slope	-2.15226E8	6.32822E6

1. High field enhancements (β) can field emission.
2. Low work function (ϕ_0) in small areas can cause field emission.

typical picture ➔
geometric perturbations (β)

alternate picture ➔
material perturbations (ϕ_0)

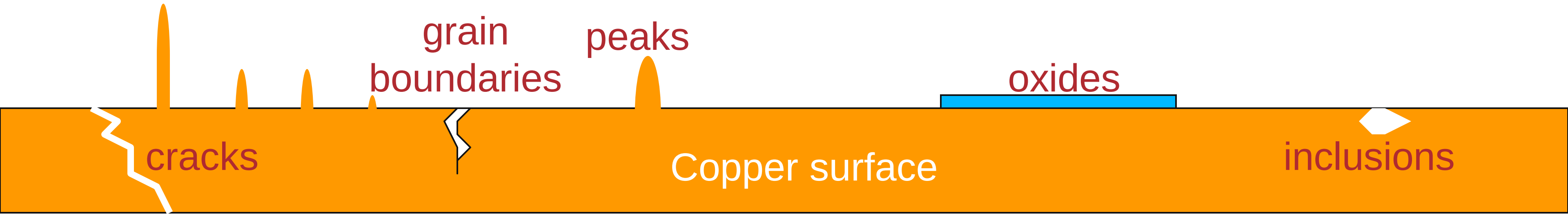

(suggested by Wuensch and colleagues)

Schottky Enabled Photo-electron Emission Measurements

Data 2010-10-04

First results from Tsinghua

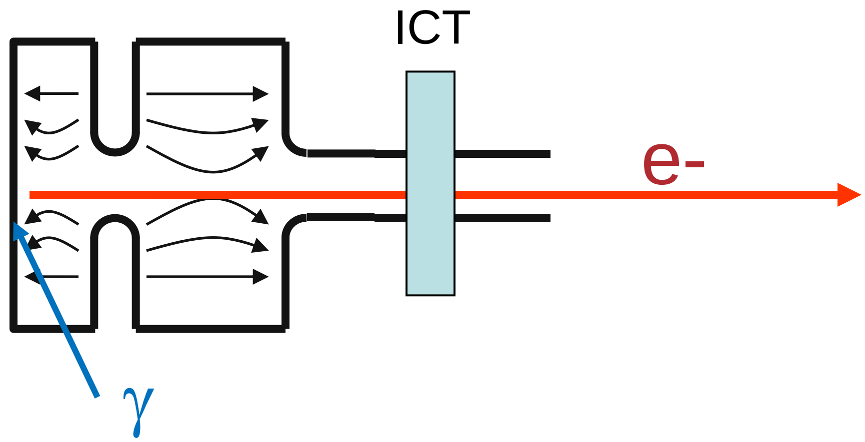

Should not get photoemission

- **Experimental parameters**
  - work function of copper = ϕ_0 = 4.65 eV
  - energy of λ=400nm photon = hν= 3.1 eV
  - Laser pulse length
    - *Long = 3 ps*
    - *Short = 0.1 ps*
  - Laser energy ~1 mJ (measured before laser input window)
  - Field (55 – 70 MV/m)

First results from Tsinghua

Data 2010-10-04

→Long Laser Pulse (~ 3ps)
→E=55 MV/m@ injection phase=80 → 55sin(80)=54

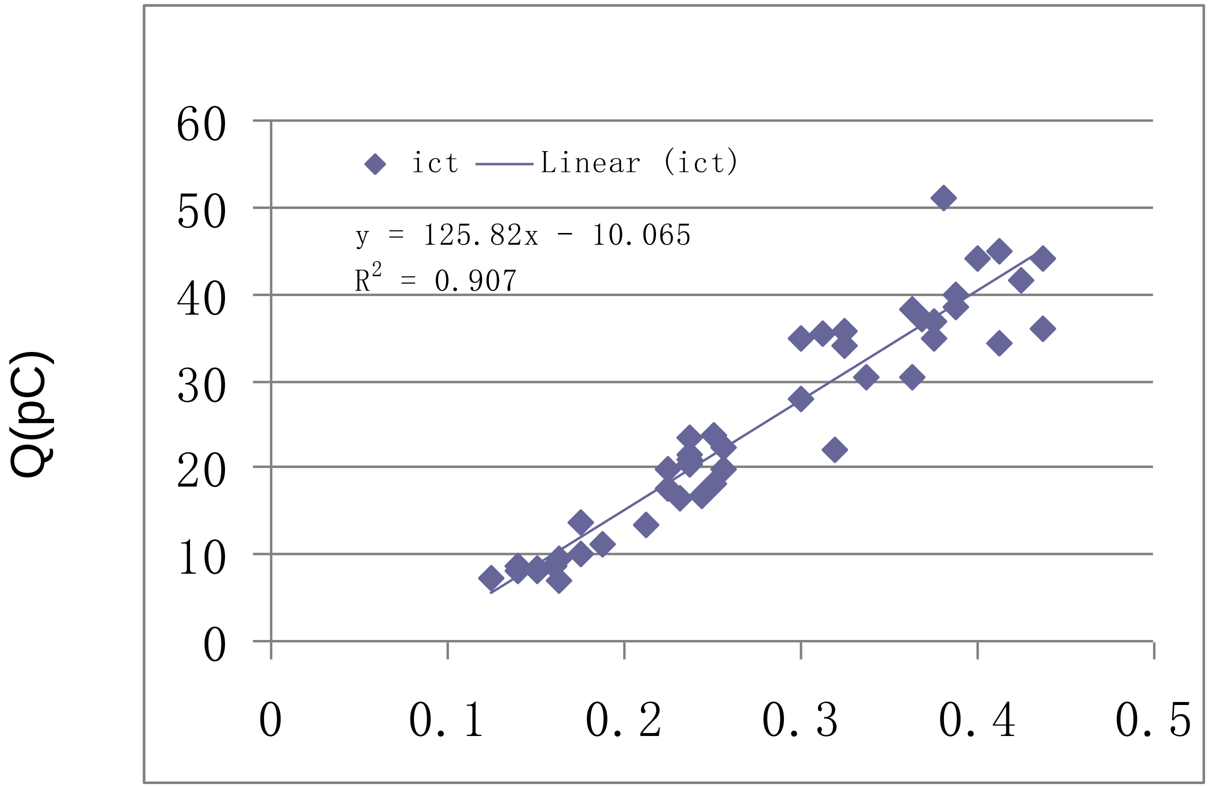

laser energy (mJ)
photocathode input window

Q ∝ I
single photon emission

Results of the recent work

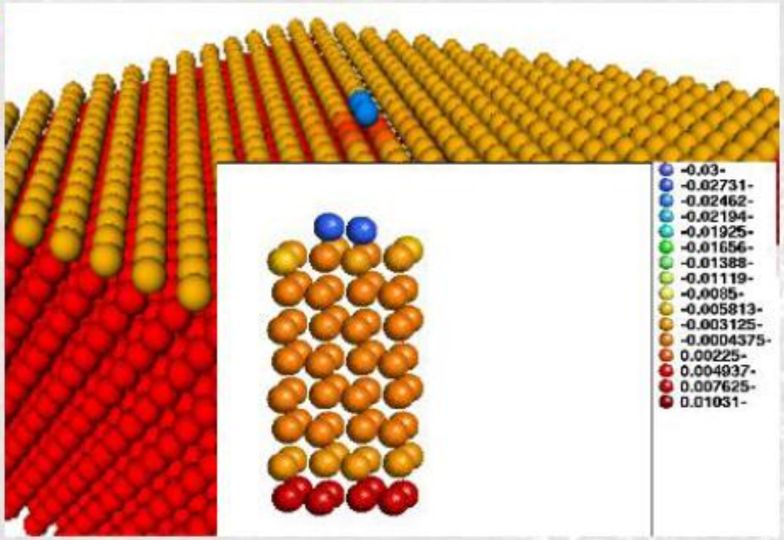

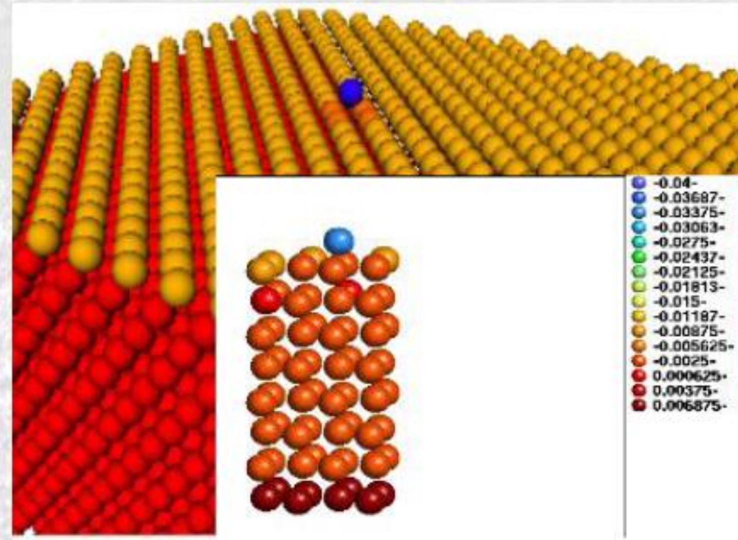

	Single adatom		Two adatoms	
	DFT	ED-MD	DFT	ED-MD
Partial Charge, q_e	-0.032	-0.0215	-0.025	-0.0177

	Flat surface		Surface with one adatom
	present DFT	experiment [16]	
Work function, eV	4.61	4.46 ± 0.03	4.30

Modelling DC discharges

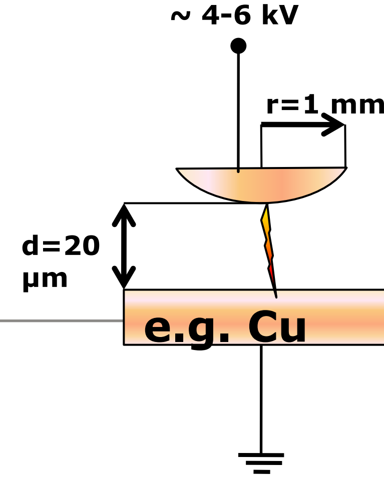

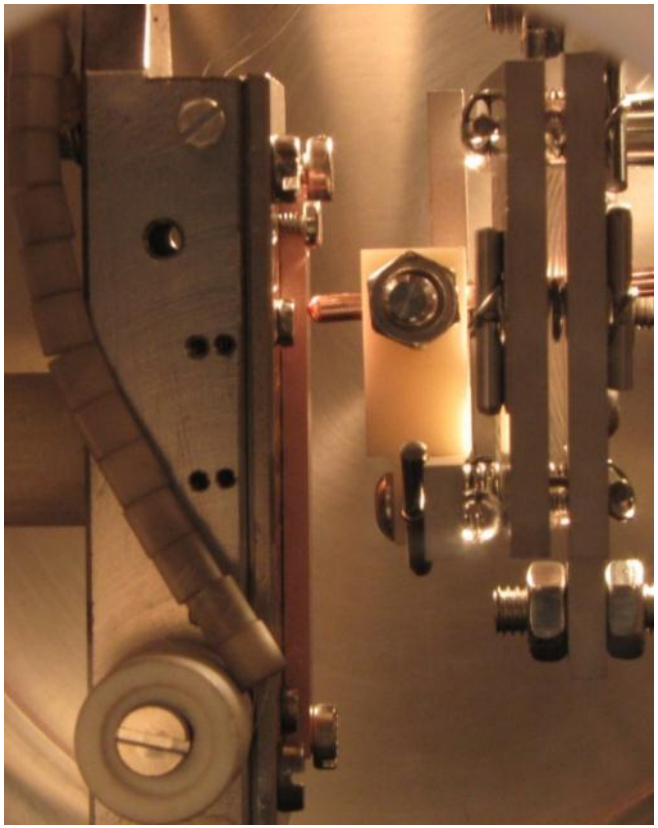

- First we have to understand breakdowns in DC, before we can generalise to RF
- Simple and cost-efficient testing of breakdown behaviour with two *DC setups at CERN*
  - We adjusted also out theoretical model to the DC experimental conditions

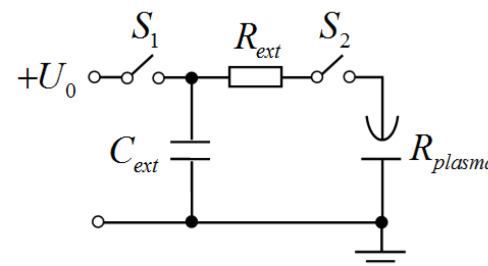

$$R_{ext} = 30\Omega$$

$$C_{ext} = 0.1 - 27.5nF$$

- However, results are completely general!

Evolution of β & E_b during conditioning experiments

- Measurements of β after each sparks (Cu electrodes)

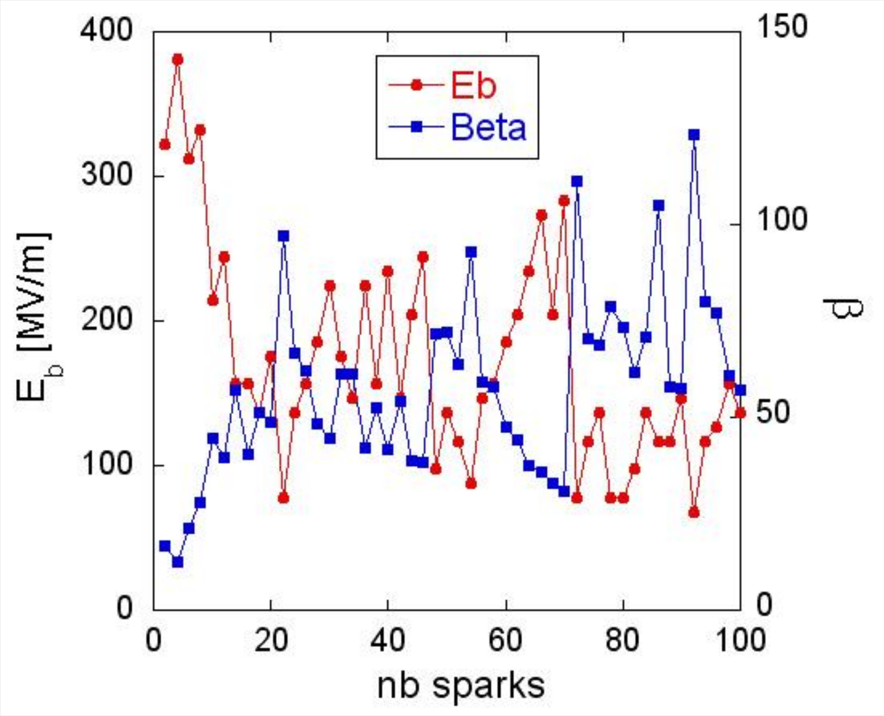

β ↔ next E_b **correlation**

$\beta \cdot E_b$ = cst

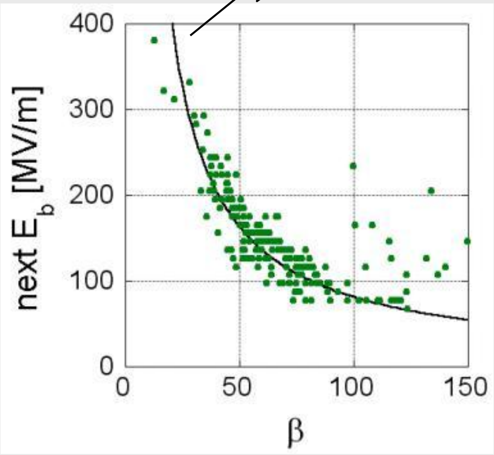

β ↔ previous E_b **no correlation**

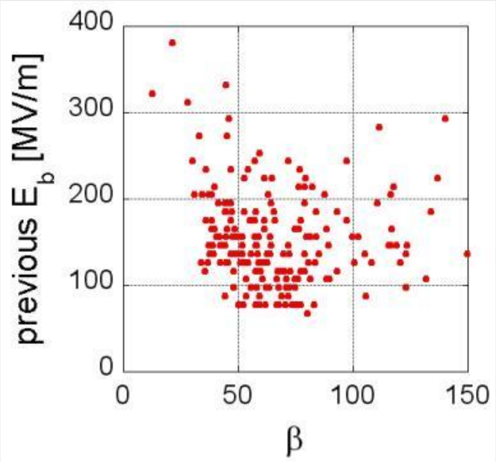

Evolution of β during BDR measurements (Cu)

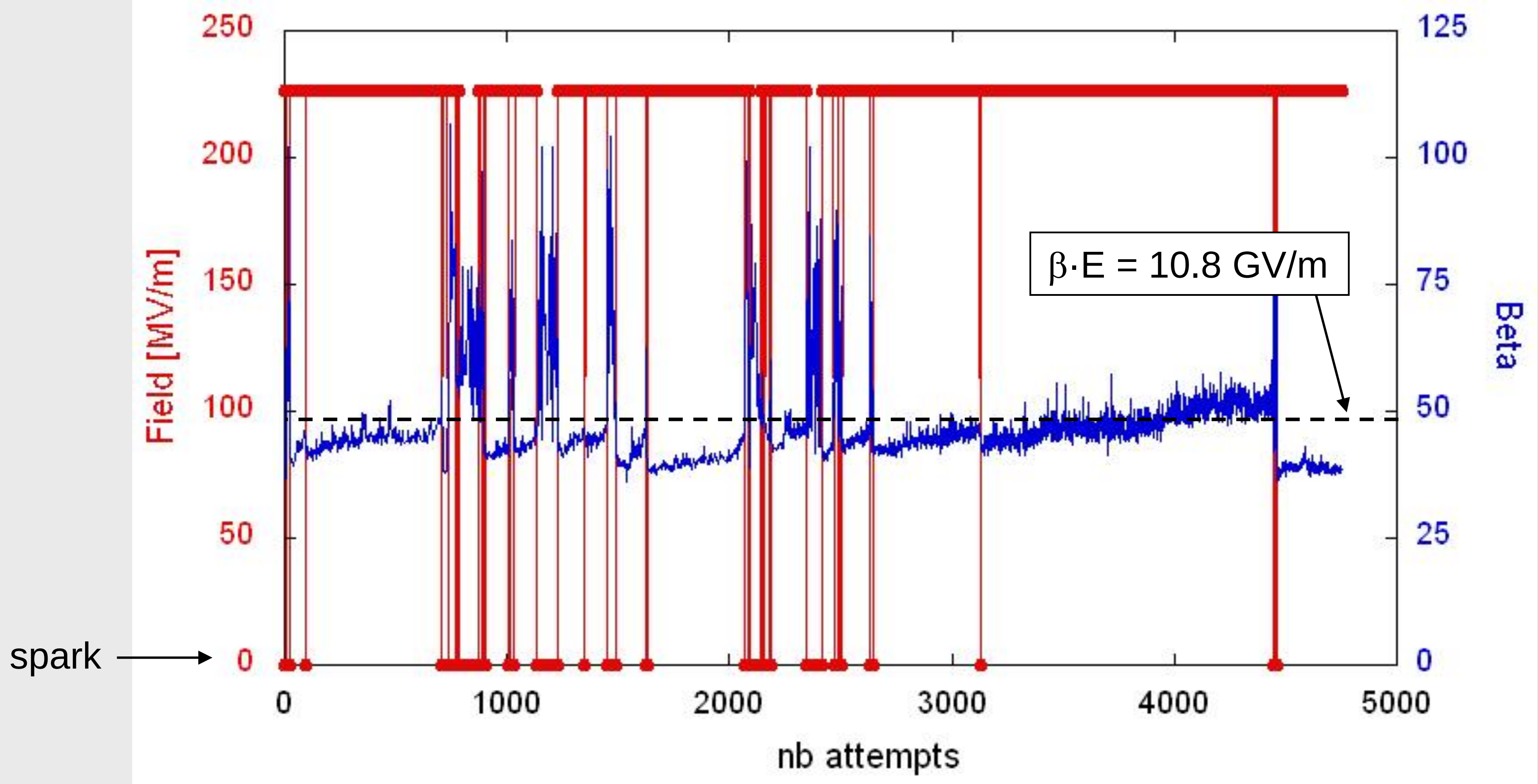

- breakdown as soon as $\beta > 48$ ($\leftrightarrow$ $\beta \cdot 225$ MV/m > 10.8 GV/m)
- consecutive breakdowns as long as $\beta > \beta_{threshold}$

→ length and occurence of breakdown clusters $\leftrightarrow$ evolution of β

What are the field emitters? Why do we look for dislocations?

- The dislocation motion is strongly bound to the atomic structure of metals. In FCC (face-centered cubic) the dislocation are the m and HCP (hexagonal close-packed) are the hardest for dislocat mobility.

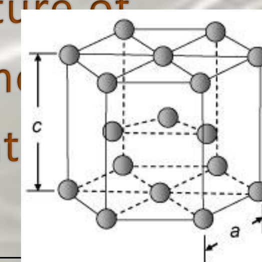

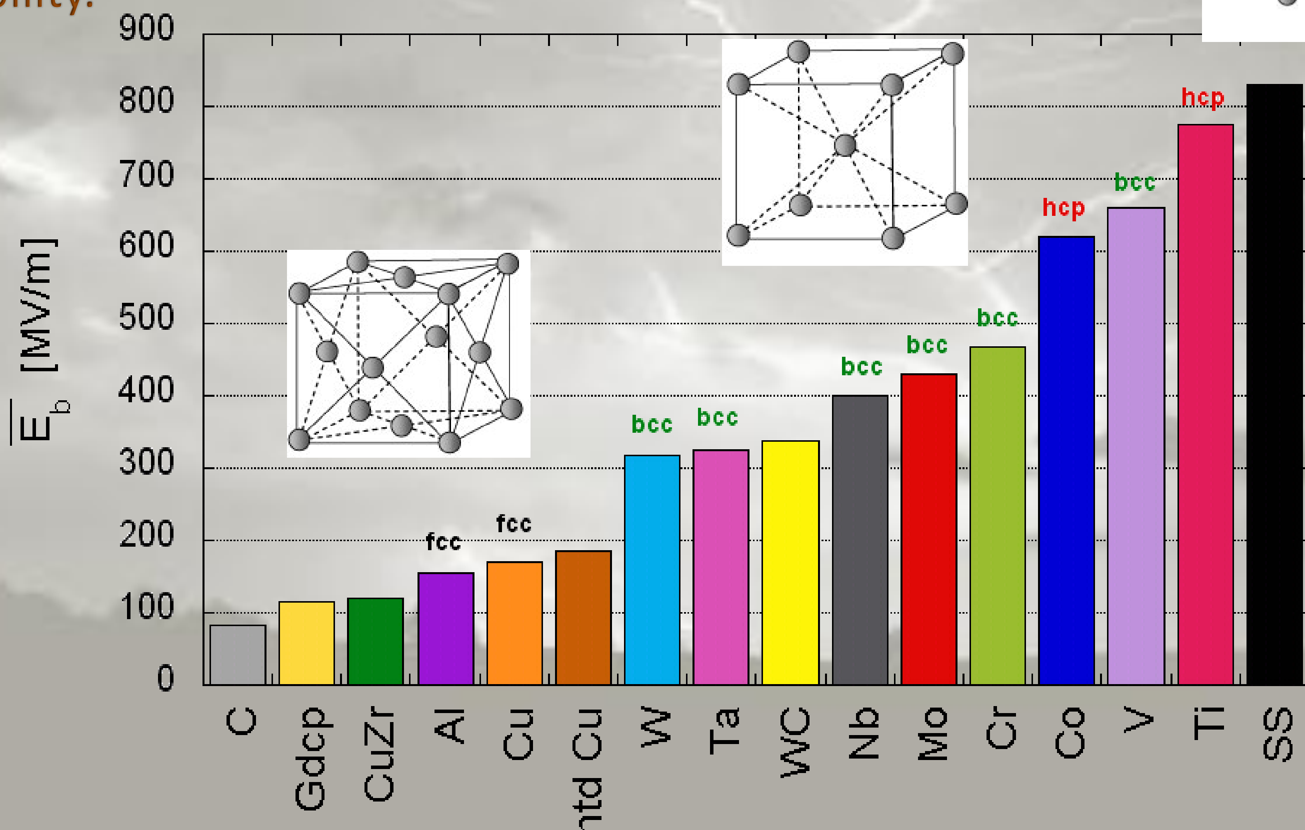

A. Descoeudres, F. Djurabekova, and K. Nordlund, DC Breakdown experiments with cobalt electrodes, CLIC-Note XXX, 1 (2010).

Dislocation-based model for electric field dependence

- Now to test the relevance of this, we fit the experimental data
- The result is:

$$BDR \propto c_0 e^{-(E^f - \varepsilon_0 E^2 \Delta V)/kT} = c_0 e^{-E^f/kT} e^{\varepsilon_0 E^2 \Delta V / kT}$$

Power law fit

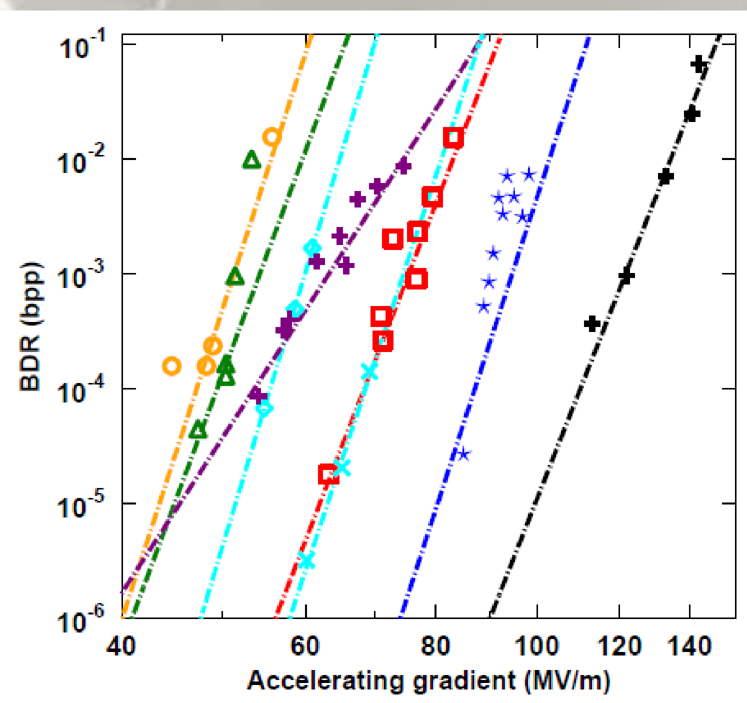

Stress model fit

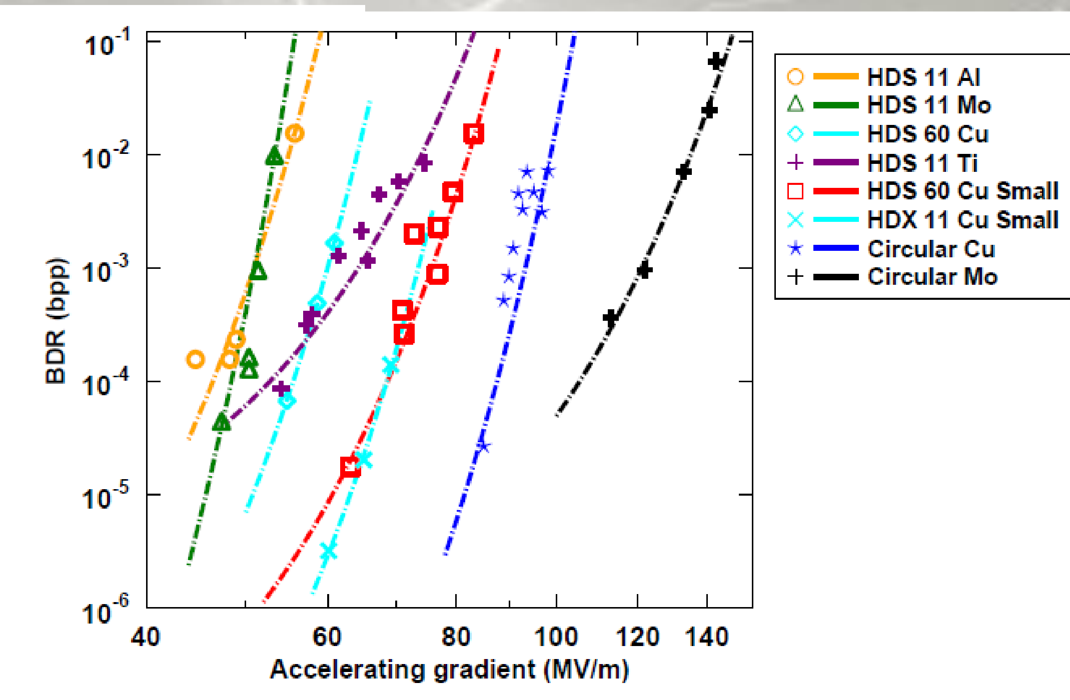

[W. Wuensch, public presentation at the CTF3, available online at http://indico.cern.ch/conferenceDisplay.py?confId=8831.] with the model.]

Observations

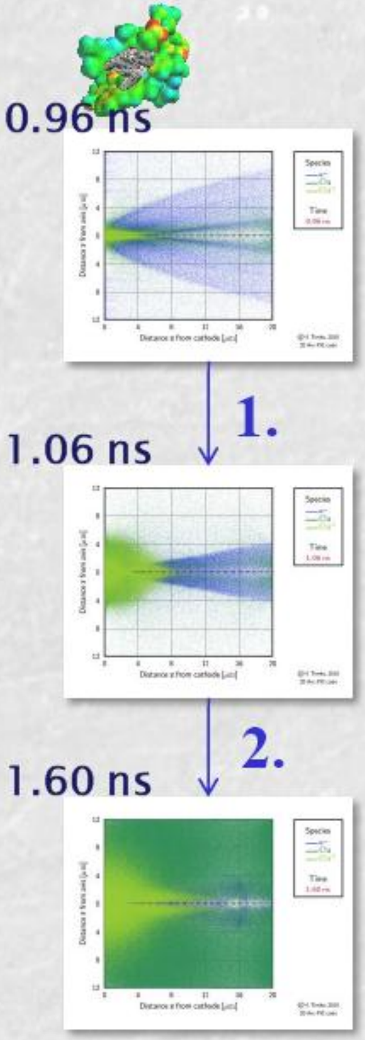

- Fully cathode dominated phenomenon
- Although FE starts from a small area, the discharge plasma can involve a macroscopic area on the cathode
- Transitions seen:
  1. Transition from strong FE to a small discharge plasma
     - Sudden ionisation avalanche
     - A plasma sheath forms, the plasma becomes quasi-neutral
     - Focusing effect
  2. Transition from a surface-defined phase to a volume-defined phase
     - When neutrals fill the whole system
     - Self-maintaining
     - Macroscopic damage

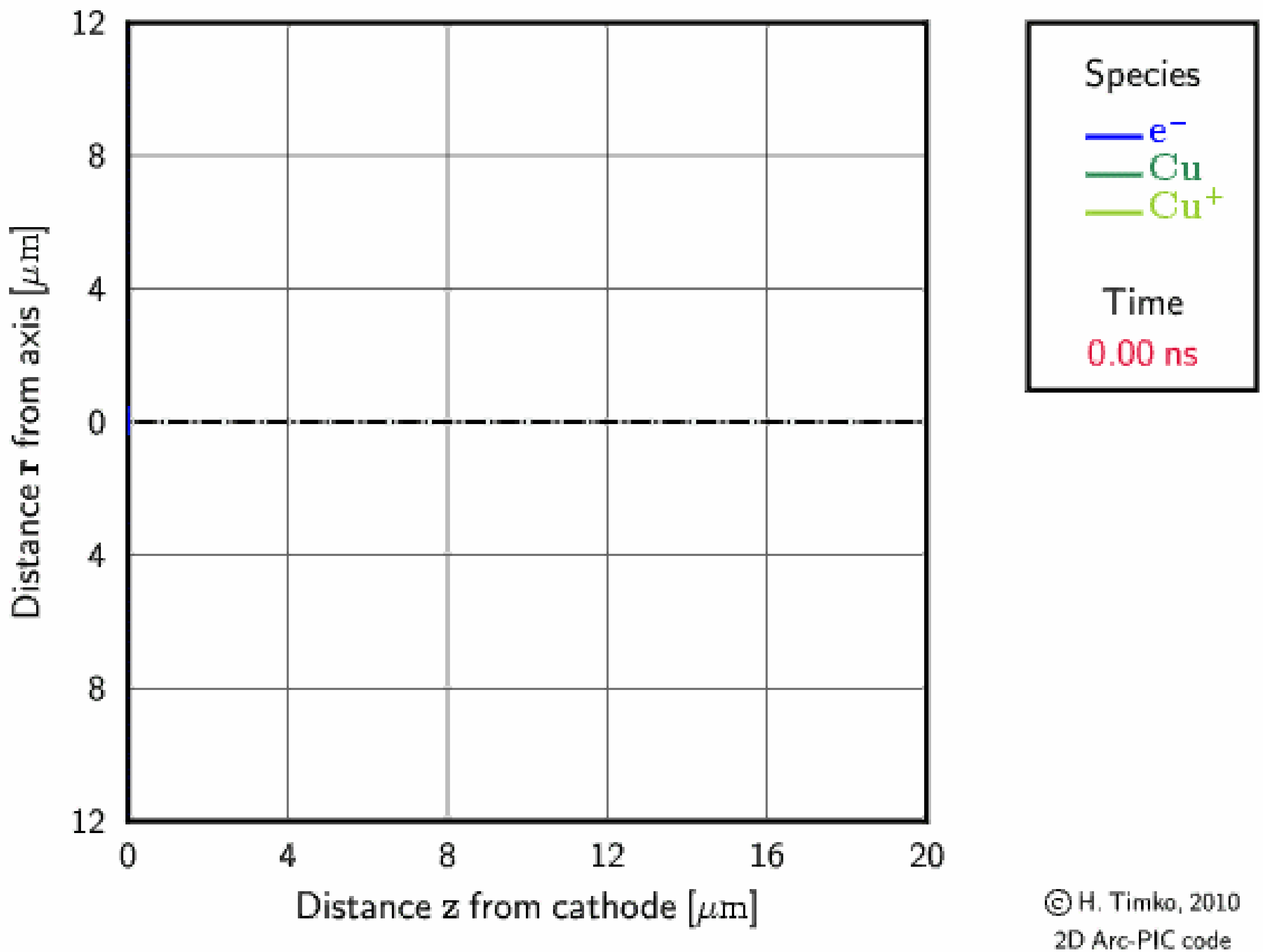
12
8
4
0
4
8
12
Distance r from axis [μm]
0
4
8
12
16
20
Distance z from cathode [μm]
Species
e⁻
Cu
Cu⁺
Time
0.00 ns
© H. Timko, 2010
2D Arc-PIC code

TD24 Pulsed surface heating limit

Cell # (cell #1 is a input matching cell):

4 5 6 7 8 9 10 11 12 13 14 15 ?16? 17 18 Last regular cell: 19

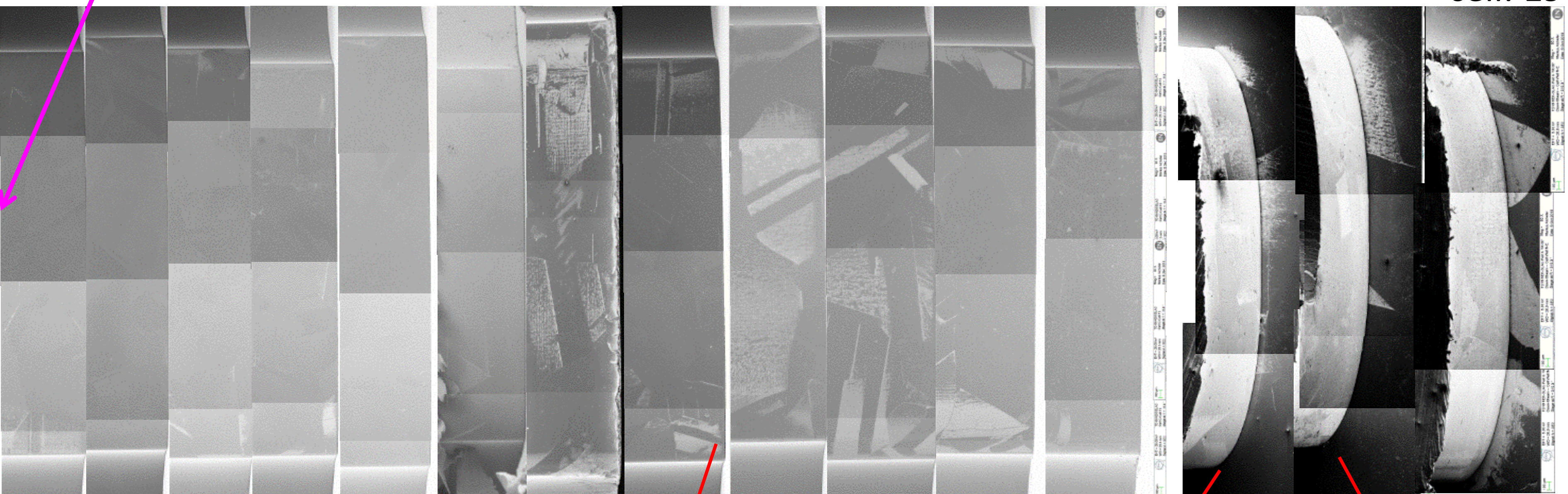

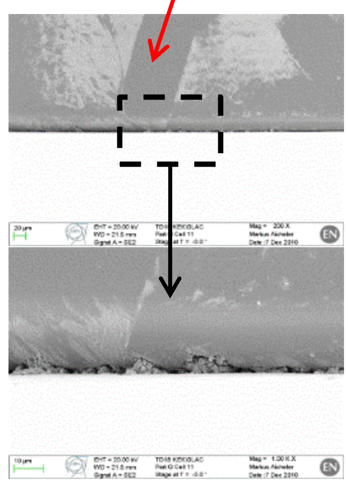

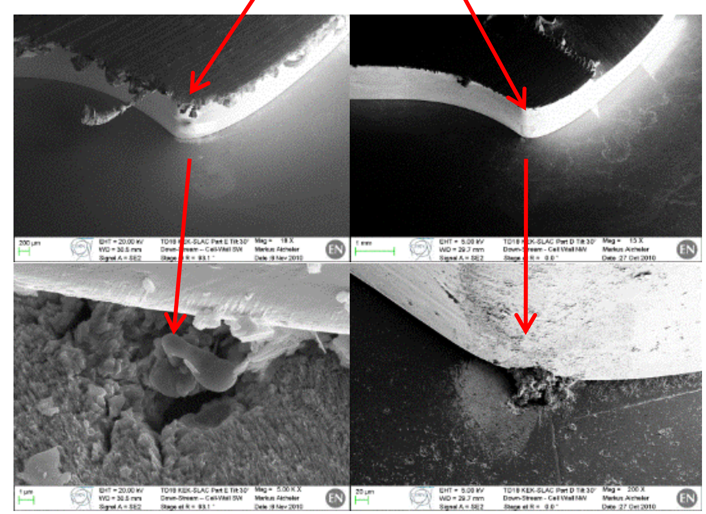

It seems that cell #10 (regular cell #9 ~ **middle cell**) exhibits the level of damage which could be considered as **a limit.**

A. Grudiev

Images courtesy of M. Aicheler: http://indico.cern.ch/getFile.py/access?contribId=0&resId=1&materialId=slides&confId=106251

Accelerating structures – manufacture

Stacking disks

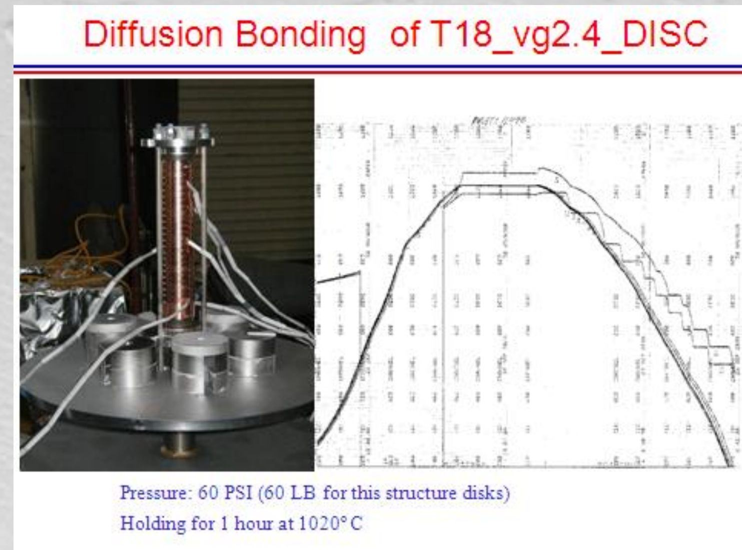

Temperature treatment for high-gradient

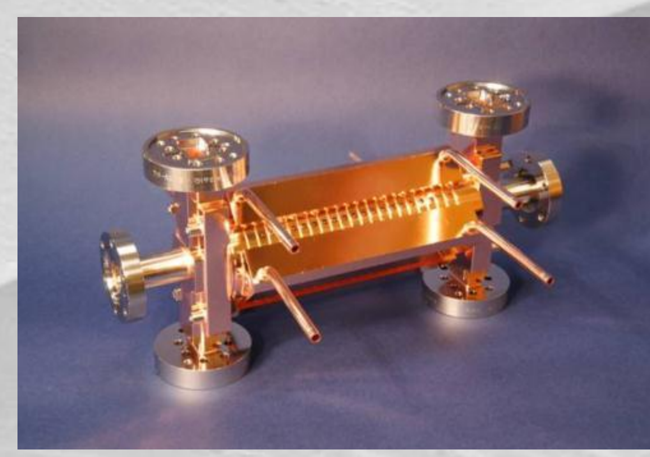

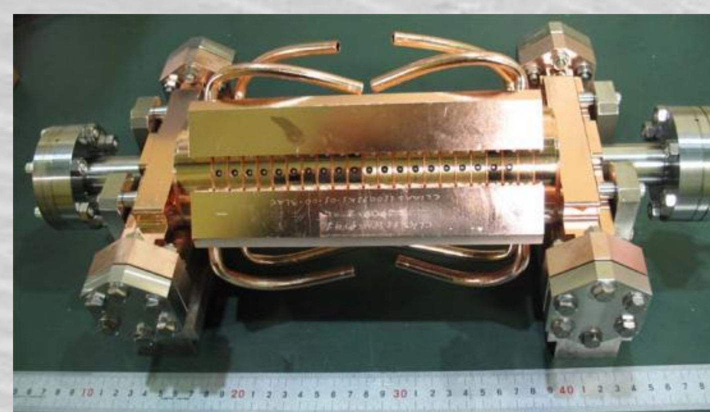

Structures ready for test

Possible applications

We can identify other applications which would benefit from high-gradient technology:

- Linacs for proton and carbon ion cancer therapy.
- High repetition rate FELs (Free Electron Lasers) for the 'photon-science' community. Users of these machines encompass biology, chemistry, material science and many other fields.
- Compton-scattering gamma ray sources providing MeV-range photons for laser-based nuclear physics (nuclear-photonics) and fundamental processes (QED studies for example). There are also potential applications such as nuclear resonance fluorescence for isotope detection in shipping containers and mining.
- Classical industrial linacs.

The End

More information:

CLIC: http://clic-study.org/
Linear collider workshop:
http://www.uta.edu/physics/lcws12/pages/registration.html
Breakdown physics:
http://www.regonline.com/builder/site/Default.aspx?EventID=1065351
High-gradient structures:
https://indico.cern.ch/conferenceDisplay.py?confId=165513
Further applications:
https://indico.desy.de/conferenceDisplay.py?confId=6537